



GRADO EN INGENIERÍA EN TECNOLOGÍAS DE TELECOMUNICACIÓN

TRABAJO FIN DE GRADO

CREATION OF A WEIGHING GRAPPLE BASED ON TECHNOLOGY PRINTED ELECTRONICS, OPERATING BY RADIO LINK

Autor: Marina Martín Cadahía

Director: Pierre-Jean Cottinet

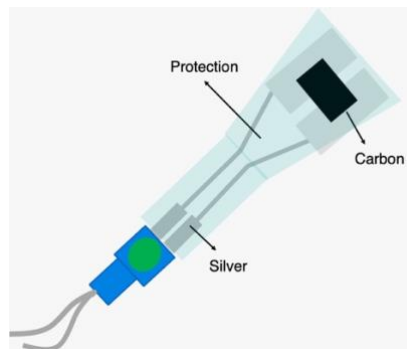
Co-Director: Elsa Dos Santos

Madrid

Julio 2024

FINAL DEGREE PROJECT

CREATION OF A WEIGHING GRAPPLE BASED ON
TECHNOLOGY
PRINTED ELECTRONICS, OPERATING BY RADIO LINK



Author: Marina Martín Cadahía

Director: Pierre-Jean Cottinet

Co-Director: Elsa Dos Santos

Madrid

July 2024

I declare, under my responsibility, that the Project presented with the title
**CREATION OF A WEIGHING GRAPPLE BASED ON TECHNOLOGY
PRINTED ELECTRONICS, OPERATING BY RADIO LINK**

at the ETS of Engineering - ICAI of the Universidad Pontificia Comillas

in the academic year 2023/24 is my own work, original and unpublished,

and has not been submitted previously for any other purposes.

The Project is not a plagiarism of another,

either in whole or in part, and the information taken from other

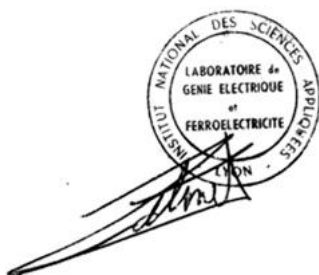
documents is properly referenced.



Signed: Marina Martín Cadahía Date: 10/ 07/ 2024

Project delivery authorized

THE PROJECT SUPERVISOR



Signed: Pierre-Jean Cottinet Date: 26 / 07 / 2024



GRADO EN INGENIERÍA EN TECNOLOGÍAS DE TELECOMUNICACIÓN

TRABAJO FIN DE GRADO

CREATION OF A WEIGHING GRAPPLE BASED ON TECHNOLOGY PRINTED ELECTRONICS, OPERATING BY RADIO LINK

Autor: Marina Martín Cadahía

Director: Pierre-Jean Cottinet

Co-Director: Elsa Dos Santos

Madrid

Julio 2024

Acknowledgements

I want to thank Jean-Pierre Cottinet and Elsa Dos Santos who have guided me through this project, as well as Derisys and AEC in partnership with INSA Lyon to have given me the opportunity to work with them.

Also, I would like to give a special thank you to my family, whose support have been essential in all this process.

CREACIÓN DE UNA PINZA DE PESAJE BASADA EN TECNOLOGÍA DE ELECTRÓNICA IMPRESA, OPERANDO POR ENLACE DE RADIO

Autor: Martín Cadahía, Marina

Supervisores: Cottinet, Pierre-Jean; Dos Santos, Elsa

Entidad colaboradora: INSA Lyon, Derysis, ArcenCiel sérigraphie

RESUMEN DEL PROYECTO

En este proyecto, se probarán tres sensores con el fin de determinar el más adecuado para usar en la creación de una pinza de pesaje basada en tecnología de electrónica impresa. Además, se diseñará un primer prototipo de la placa de circuito impreso, para que sea impresa en la garra.

1. Introducción

El trabajo presentado en este informe se realiza para la creación de una garra de pesado (Ilustración 1), que es un proyecto real propuesto por la empresa Derisys. Los sensores utilizados para la garra de pesado están basados en la serigrafía, una tecnología que proporciona mejor eficiencia ya que el consumo de energía es muy bajo (bajo voltaje requerido), y un diseño pequeño que facilita su impresión en el material de la garra.



RMT -XW GRAPPLE SCALES, RECYCLING TODAY

Ilustración 1: Pinza de pesaje comunicando el peso a un dispositivo

2. Definición del proyecto

El objetivo de esta parte del proyecto es caracterizar tres sensores proporcionados por ArcenCiel sérigraphie, realizados mediante tecnología de serigrafía, para determinar cuál de ellos responde mejor bajo diferentes factores de tensión, humedad, temperatura y envejecimiento. El sensor elegido será el que utilizaremos en el diseño final de la PCB (el circuito impreso).

Estos sensores fueron diseñados para sustituir los sensores en forma de S utilizados hasta ahora en la industria. También miden la deformación, pero son mucho más voluminosos y difíciles de colocar en la garra, mientras que los sensores serigrafiados ofrecen un producto ligero y fácil de instalar. Estos están hechos de varias tintas, como plata y carbono, esta última posee propiedades que le permiten cambiar su conductividad (resistencia eléctrica) dependiendo de la deformación del material donde está fijada.

3. Descripción de las herramientas y recursos utilizados

Debido a que es un proyecto práctico, se utilizaron muchos recursos para las diferentes pruebas realizadas, incluyendo una máquina de estrés mecánico y una cámara de temperatura y humedad. La primera se utilizó para el cálculo del factor de deformación (gauge factor), que indica cómo el sensor responde a la deformación en relación con el cambio en su resistencia eléctrica. La segunda se utilizó para las pruebas de temperatura, envejecimiento térmico y deriva de humedad.

Todos los datos se recopilaron utilizando un DEWE, un dispositivo que es capaz de obtener las mediciones cambiantes de la resistencia de los sensores en tiempo real. Todo el material adicional necesario para los ensayos de laboratorio desde las muestras de acero y los sensores de calibración (para medir temperatura y deformación) hasta los cables de conexión fueron proporcionados por INSA Lyon.

4. Resultados

En primer lugar, observamos una disminución de la resistencia en el ensayo de temperatura, con tendencia a mantenerse constante. Esto llevó a pensar que una prueba de envejecimiento térmico sería necesaria para ver si esta resistencia se estabilizaba, lo cual puede ser útil para determinar si es necesario un proceso de acondicionamiento mediante envejecimiento del sensor antes de su uso.

En segundo lugar, en la prueba de deformación mecánica, determinamos que el sensor 1 era el ideal para hacer el circuito impreso, este sensor tenía un buen factor de deformación de 2.26, parecido a los factores que tienen los materiales metálicos. La Ilustración 2 muestra la respuesta de este sensor en función de un sensor comercial, utilizado para comparar el cambio en la resistencia según el cambio de voltaje en el circuito, que pasa por la resistencia del sensor.

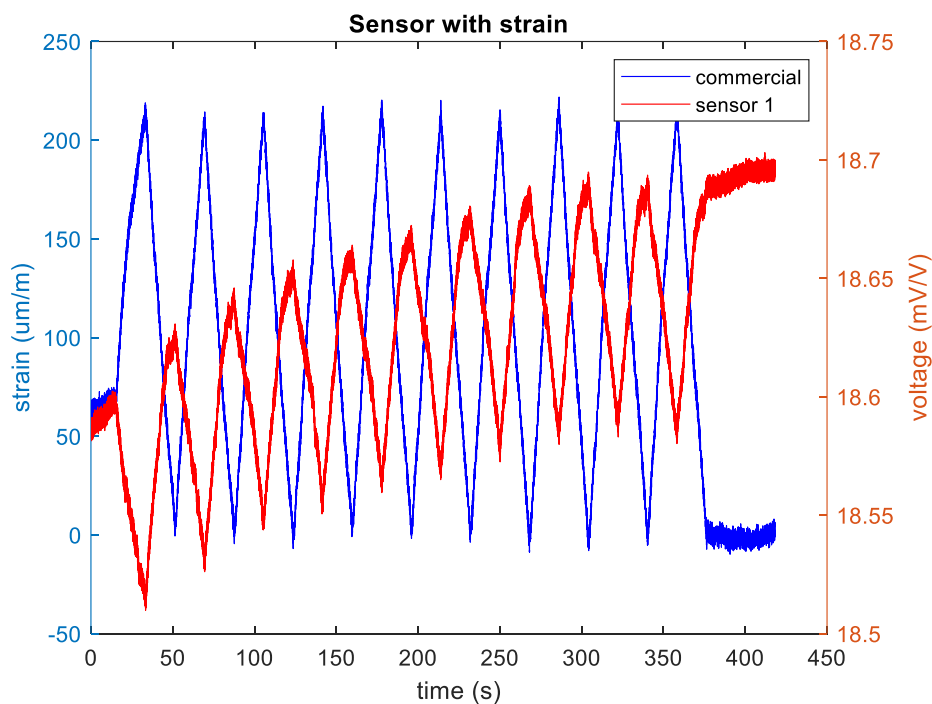


Ilustración 2: Resistencia en función del tiempo y deformación en función del tiempo

La tendencia del sensor 1 era cada vez más constante, por lo que necesitábamos hacer un envejecimiento térmico para ver esta progresiva estabilización. Obtenemos los resultados de la Ilustración 3, que muestra que la resistencia se mantiene después de unas horas, lo que significa

que podría ser necesario realizar un envejecimiento térmico del sensor antes de su uso. También podemos ver una pequeña deriva térmica que necesitaríamos tener en cuenta en el diseño final.

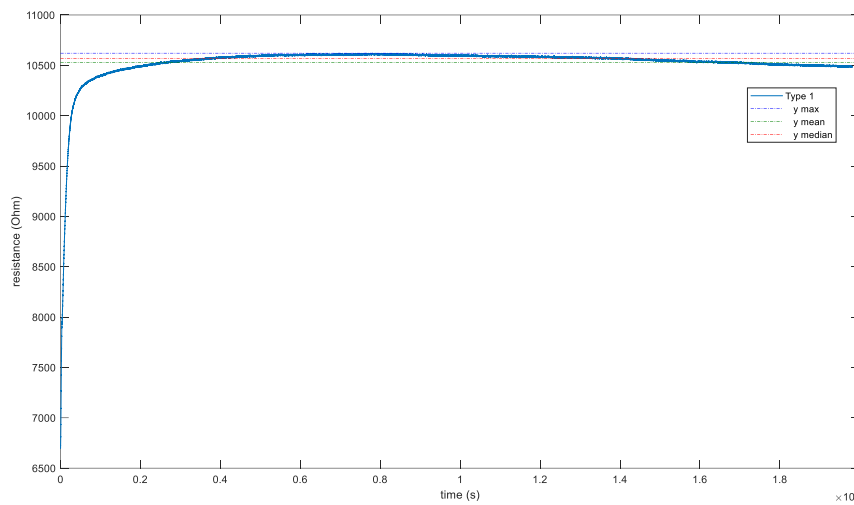


Ilustración 3: Respuesta al envejecimiento (48 horas a 80°C)

Donde: $Y_{max}=10.620 \Omega$ $Y_{mean}=10.530 \Omega$ $Y_{median}=10.570 \Omega$

Luego, realizamos la prueba de deriva de humedad, cuyos resultados se muestran en la Ilustración 4. Observamos un aumento en la resistencia y luego estabilización. Según los datos, puede ser necesaria una compensación de la deriva de humedad.

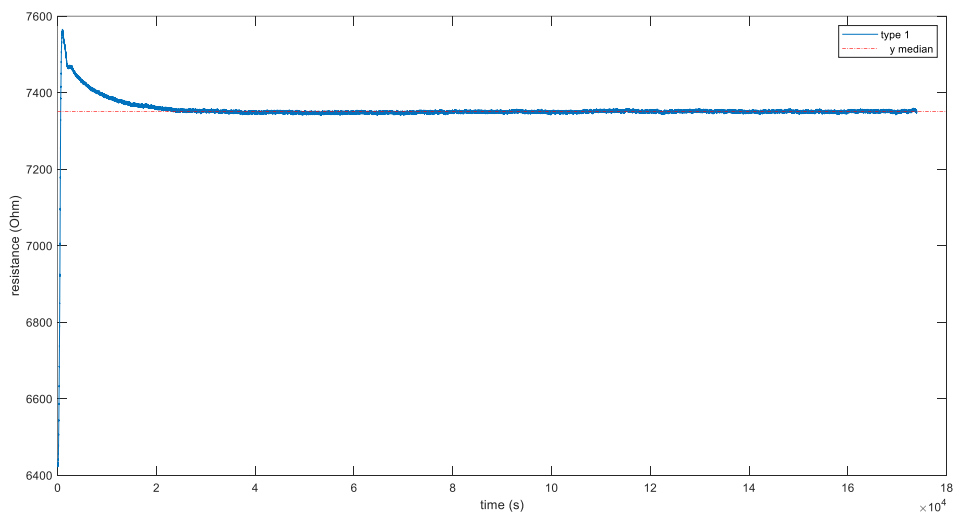
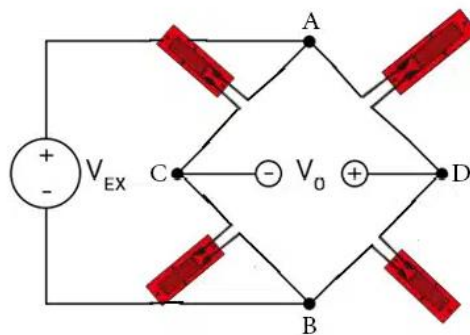


Ilustración 4: Respuesta del sensor 1 bajo el test de humedad

Donde Y_{median} is 7350Ω y la respuesta se estabiliza a aproximadamente $30000s \approx 8$ hours.

Por último, hicimos un primer diseño de la placa de circuito impreso utilizando el software ALTIUM, considerando todos los datos recopilados. El diseño (Ilustración 6) tenía dos aspectos críticos:

- Configuración de **punto de Wheatstone** (Ilustración 5): cuatro de estos sensores (en rojo) están configurados en un puente de Wheatstone completo. Hacer esta configuración asegura una mejor compensación de temperatura y precisión en las mediciones de deformación.



BESTECH: SENSORS AND TEACHING EQUIPEMENT, FULL WHEATSTONE BRIDGE

Ilustración 5: Configuración de puente de Wheatstone completo

- Componente **MAX1452**: debido a la deriva térmica, es obligatorio agregar el MAX1452 en el circuito, para compensar el cambio en la resistencia causado por el cambio de temperatura.

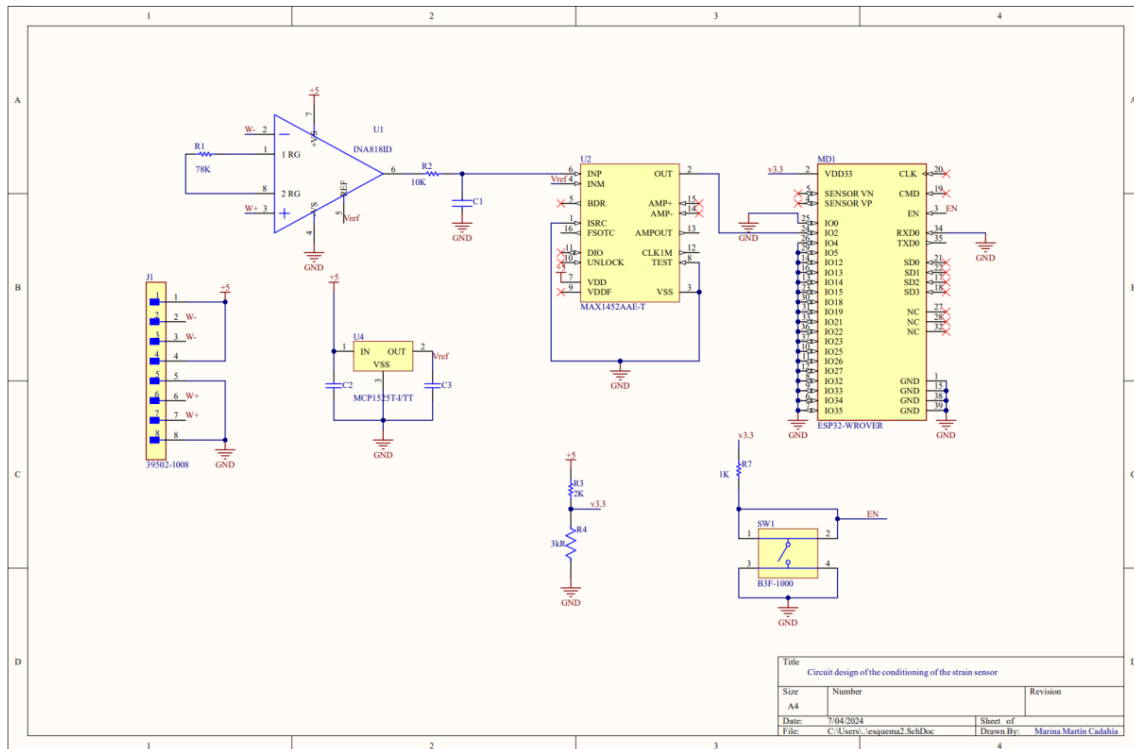


Ilustración 6: Diseño esquemático de la PCB

5. Conclusiones

La serigrafía ofrece un avance tecnológico en el mundo de los sensores y la electrónica impresa. La capacidad del carbono para cambiar su conductividad permite depositar la tinta de carbono directamente sobre la garra de pesado (por serigrafía), al igual que el circuito impreso que procesa la variabilidad de su resistencia y envía la señal al dispositivo correspondiente, el cual muestra el peso transportado por el gancho.

Se necesitarán pruebas apropiadas para caracterizar el sensor, determinando su respuesta ante diferentes factores que tomaremos en cuenta en el diseño final, como la deriva térmica.

Además, estos sensores se definen por su factor de deformación, que mide su dependencia de la resistencia a la deformación del material. En este caso, obtuvimos un valor de 2,26, que es ideal para nuestra aplicación pero que puede disminuir con la temperatura y la humedad.

Para futuras mejoras, podríamos necesitar realizar más ciclos de pruebas de humedad y pruebas de envejecimiento térmico, para analizar más profundamente las pequeñas variaciones del

factor de deformación bajo las diferentes condiciones de temperatura y humedad. Además, es importante añadir al diseño electrónico, las últimas especificaciones solicitadas por Derisys, como el módulo conectado a la antena para enviar los datos por enlace de radio al dispositivo que mostrará el peso.

6. Referencias

[MGFE24] McGill Formula Electric, Compact Strain Gauge Board for MFE22, Canada. April 2022. Last accessed on 12/07/2024. <https://www.hackster.io/MFE/compact-strain-gauge-board-for-mfe22-113dd5>

[ANAL04] Analog Devices, Driving Strain-Gauge Bridge Sensors with Signal-Conditioning ICs. December 2004. Last accessed on 12/07/2024. <https://www.analog.com/en/resources/technical-articles/driving-straingauge-bridge-sensors-with-signalconditioning-ics.html>

[ELPR24] Electronics, Projects, Focus (ELPROCUS), Types of Strain Gauge : Characteristics & Its Applications. Last accessed on 12/07/2024. <https://www.elprocus.com/types-of-strain-gauge/>

CREATION OF A WEIGHING GRAPPLE BASED ON TECHNOLOGY PRINTED ELECTRONICS, OPERATING BY RADIO LINK

Author: Martín Cadahía, Marina

Supervisors: Cottinet, Pierre-Jean; Dos Santos, Elsa

Colaborating entitiy: INSA Lyon, Derysis, ArcenCiel sérigraphie

ABSTRACT

In this project, three sensors will be tested in order to determine the ideal one to use in the creation of a weighing grapple based on technology printed electronics. Furthermore, a first prototype of the printed circuit board is going to be designed, for it to be printed in the grapple.

1. Introduction

The work done in this report is done for the creation of a weighing grapple (Illustration 7), which is a real project proposed by the company Derisys. The sensors used for the weighing grapple are based on screen printing, a technology that provides better efficiency as the need of power is very low (low voltage needed), and a small design that facilitates its printing in the material of the grapple.



RMT -XW GRAPPLE SCALES, RECYCLING TODAY

Illustration 7: Weighing grapple communicating the weight to a device

2. Project definition

The aim of this part of the project is to characterize three sensors which are provided by ArcenCiel, done by screen printing technology, to determine which one of them responds better, to then implement it on the final PCB design.

These sensors were designed in order to substitute the S-shaped sensors used in the industry until now. They also measured the strain but are much more voluminous and difficult to place in the grapple, whereas the screen-printed sensors offer a lightweight and easy to set product. These are made of various inks, such as silver and carbon, last one possessing the properties that allows it to change its conductivity depending on the deformation of the material where it is fixed.

3. Description of the tools and resources used

Due to it being a practical project, many resources were used for the different tests done, including a mechanical stress machine and a temperature humidity chamber. The first one used for the calculation of the gauge factor, which indicates how the sensor answers to deformation in relation to the change in its conductivity. The second one was used for the temperature, thermal ageing, and humidity drift tests.

All the data has been collected by using a DEWE, a device that is able to obtain the changing measurements of the sensors in real-time. Additional material like, samples, calibration sensors (for measuring temperature and strain) or cables were provided by INSA Lyon.

4. Results

Firstly, we observed a decrease in the resistance in the temperature test. This lead to think that a thermal ageing test was going to be necessary to see if this resistance stabilized, which can be useful to determine if a preconditioning process by ageing of the sensor is necessary before use.

Secondly in the mechanical strain test, we established that sensor 1 was the ideal to do the printed circuit which had a good gauge factor of 2.26, similar to those of metallic materials.

Illustration 8, shows the response of this sensor function of a commercial sensor, used to compare the change in the resistance according to the change of voltage in the circuit, which goes by the resistance of the sensor.

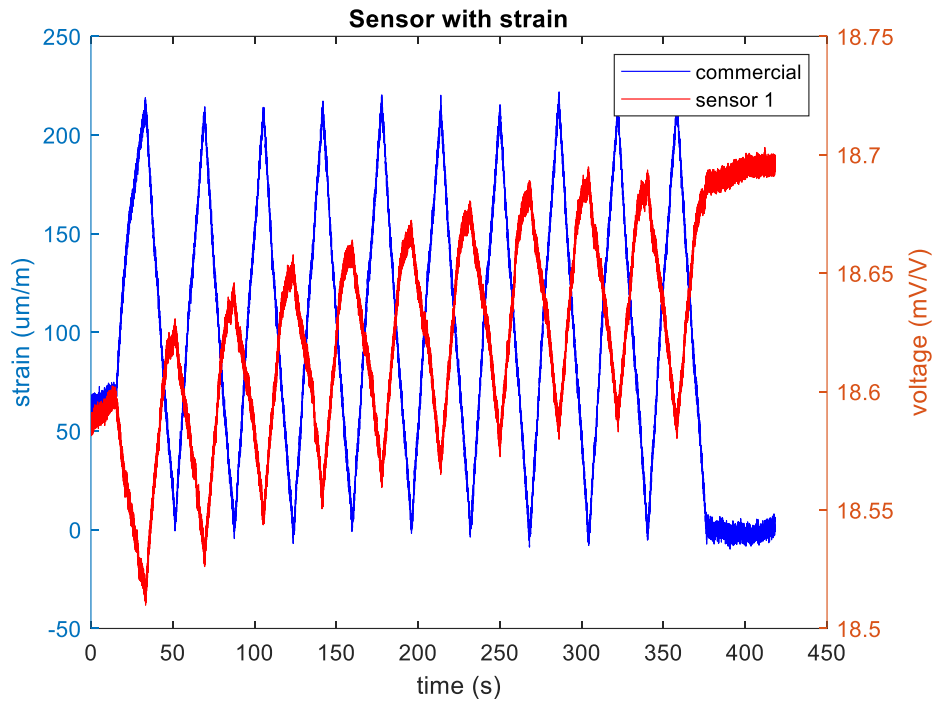


Illustration 8: Resistance function of time and strain function of time

The tendency of sensor 1 is to be more and more steady, we need to do thermal ageing to see this stabilization. We obtain the results in Illustration 9, which shows the resistance is maintained after a few hours which means that it might be necessary to do thermal ageing of the sensor before use. Also, we can see that small thermal drift that we need to take into consideration in the final design.

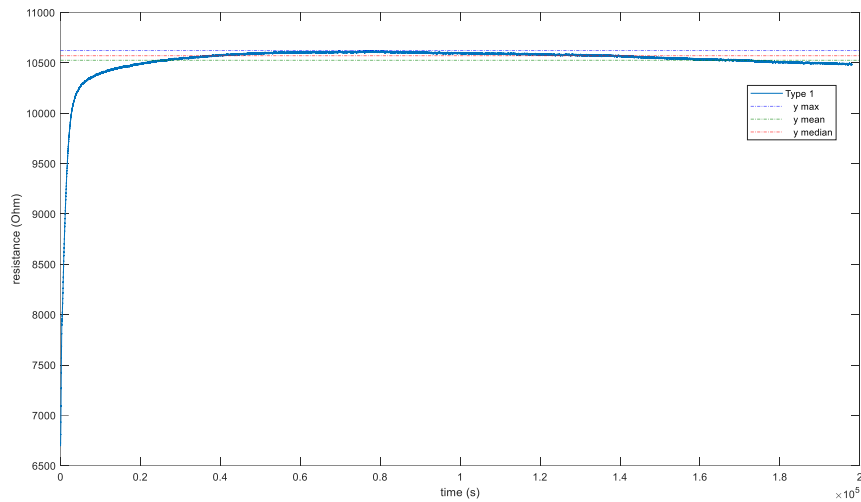


Illustration 9: Response to ageing (48 hours at 80°C)

Where: $Y_{max}=10.620 \Omega$ $Y_{mean}=10.530 \Omega$ $Y_{median}=10.570 \Omega$

Next, we did the humidity drift test, whose results are shown in Illustration 10. We observed the increase in resistance and then stabilization. According to the data, a humidity drift compensation may be necessary.

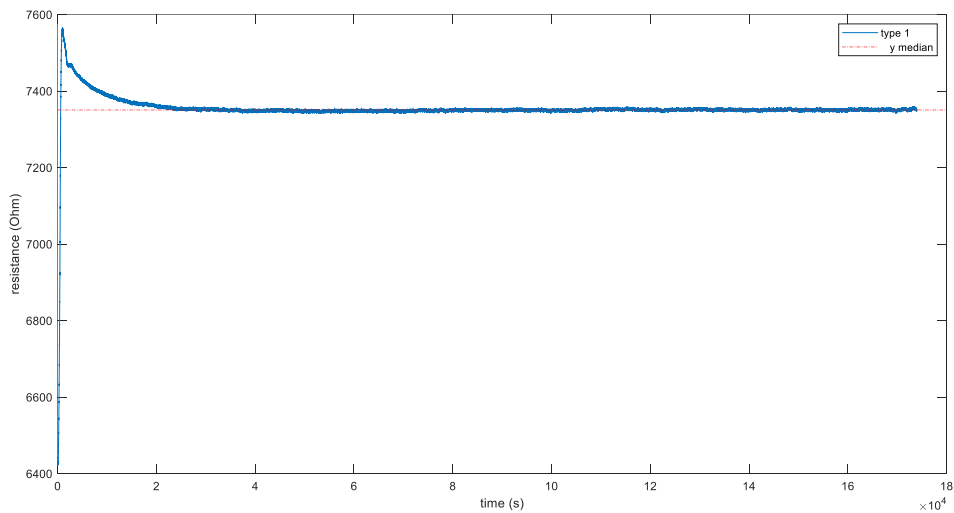
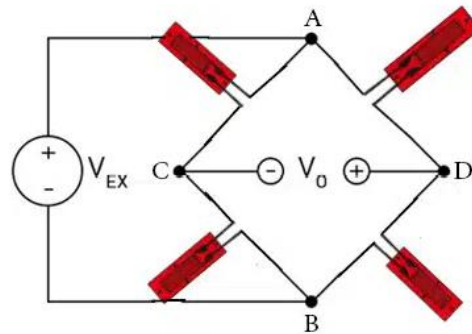


Illustration 10: Response of sensor 1 under humidity test

Where Y_{median} is 7350Ω and the response stabilises at almost $30000s \approx 8$ hours.

Lastly, we did a first design of the printed circuit board using the software ALTIUM, considering all the data gathered. The design () had two critical aspects:

- A **Wheatstone bridge configuration** (Illustration 11): four of these sensors (in red) are configured in a full Wheatstone bridge. Doing this configuration ensures better subsequent temperature compensation and precision in the deformation measurements.



BESTECH: SENSORS AND TEACHING EQUIPMENT, FULL WHEATSTONE BRIDGE

Illustration 11: Full Wheatstone bridge configuration

- A **MAX1452 component**: due to the temperature drift, it is compulsory to add the MAX1452 in the circuit, to compensate the change in the resistance caused by temperature change.

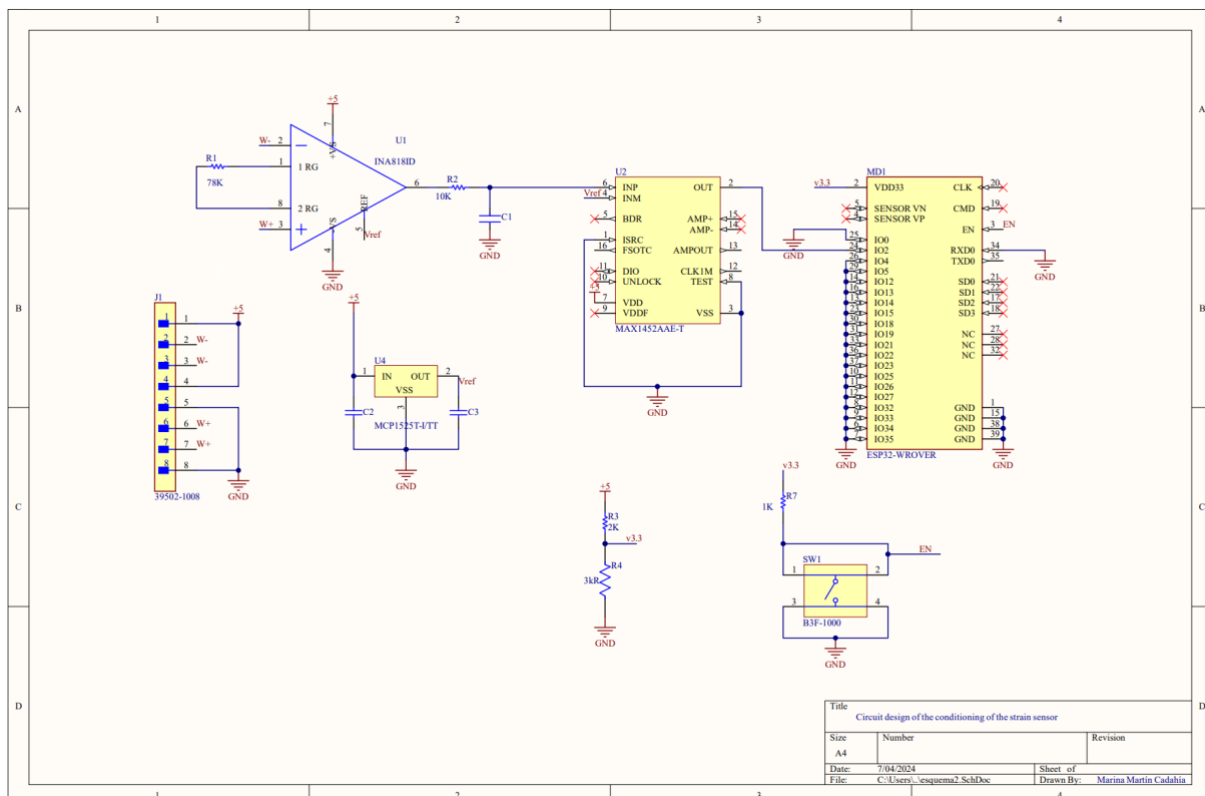


Illustration 12: Schematic design of the PCB

5. Conclusions

Screen printing offers a technological advancement in the world of sensors and printed electronics. Their ability of the carbon to change its conductivity, allows to print the carbon ink directly on the weighing grapple, as well as the printed circuit board that process the resistance variation and sends the signal to the according device, that displays the weight carried by the hook.

Appropriate tests are going to be needed in order to characterize the sensor, so to determine its response to different factors that we have taken into consideration in the final design, like the thermal drift.

Also, these sensors are defined by its gauge factor, which measures their resistance dependence to the strain of the material. In this case, we obtained one of 2.26, ideal for the application, but that also decreased with temperature and humidity.

For future improvements, we might need to do more humidity tests cycles and thermal ageing tests, to precise the small variations of the strain gauge under different conditions of temperature and humidity. Moreover, it is important to add to the electronic design, the last specifications requested by Derisys, like module connected to the antenna that sends the data by radio link to the device that shows the weight.

6. References

[MGFE24] McGill Formula Electric, Compact Strain Gauge Board for MFE22, Canada. April 2022. Last accessed on 12/07/2024. <https://www.hackster.io/MFE/compact-strain-gauge-board-for-mfe22-113dd5>

[ANAL04] Analog Devices, Driving Strain-Gauge Bridge Sensors with Signal-Conditioning ICs. December 2004. Last accessed on 12/07/2024. <https://www.analog.com/en/resources/technical-articles/driving-straingauge-bridge-sensors-with-signalconditioning-ics.html>

[ELPR24] Electronics, Projects, Focus (ELPROCUS), Types of Strain Gauge : Characteristics & Its Applications. Last accessed on 12/07/2024.
<https://www.elprocus.com/types-of-strain-gauge/>

Report index

Chapter 1. Introduction.....	1
Chapter 2. State of question	3
Chapter 3. Motivation.....	5
Chapter 4. Project objectives	6
Chapter 5. Alignment with the Sustainable Development Goals (SDG).....	7
Chapter 6. Work methodology	7
Chapter 7. Resources	9
Mechanical stress machine	10
DEWE	11
ALTIUM	12
Chapter 8. Fabrication and characteristics of sensors	13
8.1. AEC sérigraphie	13
1. Design	13
2. Sensor planification	13
3. Fabrication process	13
8.2. Screen printing	15
8.3. Sensors addressed	16
Chapter 9. Test results	17
9.1. Temperature	17
Sensor 1.....	17
Conclusion	25
9.2. Mechanical strain	25
Preparation	25
Results.....	27
Sensor 1.....	30
Sensor 2.....	32

Sensor 3.....	33
Conclusion	35
9.3. Thermal ageing	35
Conclusion	37
9.4. Humidity drift	38
Chapter 10. Circuit design	42
10.1. Schematic	42
Full bridge configuration	42
Amplifier INA8181D.....	42
MAX1452	43
Microcontroller ESP32	44
General schematic of the circuit design	45
10.2. PCB design.....	46
Chapter 11. Future improvements.....	47
Chapter 12. Conclusion	48
Chapter 13. Bibliography	49

Figure index

Figure 1: Example of a weighing grapple operating by radio link	1
Figure 2: Three types of sensors	2
Figure 3: S-shaped sensor	3
Figure 4: Three types of sensors used to measure stress.....	4
Figure 5: Gantt diagram of the working plan.....	8
Figure 6: Humidity temperature chamber.	10
Figure 7: Mechanical stress testing machine	11
Figure 8: DEWE	12
Figure 9: Steps for screen printing	15
Figure 10: screen printing using silver ink	15
Figure 11: screen printed sensor	16
Figure 12: Resistance according to temperature of sensor sample 1.1.	18
Figure 13: Resistance according to temperature of sensor sample 1.2.	18
Figure 14: chart of ΔR of sensor 1	19
Figure 15: value a of linear fit.....	19
Figure 16: Resistance according to temperature of sensor sample 2.4.	20
Figure 17: Resistance according to temperature of sensor 2.5.	21
Figure 18: chart of ΔR of sensor 2	21
Figure 19: value a of quadratic fitting.....	22
Figure 20: Resistance according to temperature of sensor 3.1.	23
Figure 21: Resistance according to temperature of sensor 3.5.	23
Figure 22: chart of ΔR of sensor 1	24
Figure 23: value a of linear fitting	24
Figure 24: mechanical strain machine	27
Figure 25: placement of the comercial sensor	27
Figure 26: configuration of the DEWE.....	29
Figure 27: Voltage variation function of strain of sensor 1.....	30
Figure 28: Resistance function of time and strain function of time.....	31
Figure 29: Voltage variation function of strain of sensor 2.....	32
Figure 30: Resistance function of time and strain function of time.....	33
Figure 31: Voltage variation e function of strain of sensor 3.....	34
Figure 32: Resistance function of time and strain function of time.....	34

Figure 33: Resistance response to thermal ageing regarding time	36
Figure 34: Resistance response to ageing regarding temperature.....	36
Figure 35: Response to ageing (48 hours at 80°C)	37
Figure 36: Temperature and humidity chamber	39
Figure 37: Sensors placed inside the chamber	39
Figure 38: Response of sensor 1 under humidity test	40
Figure 39: Humidity drift of sensors 2 and 3	41
Figure 40: amplifier INA8181D	43
Figure 41: internal structure of a MAX1452	44
Figure 42: Final schematic design	45
Figure 43: PCB, connection design	46
Figure 44: 3D design of the PCB	46

Table index

Table 1: Specifications of the design	6
Table 2: Resistance results for the sensor sample 1.1.	18
Table 3: Resistance results for the sensor sample 1.2.	18
Table 4: Resistance results for the sensor sample 2.4	20
Table 5: Resistance results for the sensor 2.5.	21
Table 6: Resistance results for the sensor 3.1.	22
Table 7: Resistance results for the sensor 3.5.	23
Table 8: Mechanical strain tests 1 and 2	28
Table 9: characteristics of a full Wheatstone bridge	42

Project Report

Chapter 1. Introduction

In this project, the company Derisys is working with ARCenCIEL Sérigraphie (AEC) to design a weighing grapple that provides real time weight information, necessary in different industrial applications like container loading and unloading. To illustrate this, we can see in Figure 1, an example of a weighing grapple operating by radio link in an industrial exploitation.



WIRELESS GRAPPLE SCALE ALLOWS SCRAP OPERATIONS TO ADD IN-MOTION WEIGH CAPACITY, RECYCLING PRODUCT NEWS

Figure 1: Example of a weighing grapple operating by radio link

The objective is to test different sensors (Figure 2,) made by screen printing, technique that is developed by AEC with INSA Lyon to then design a printed circuit board, that will transmit the data by radio link to another device, that will show the weight. The aim is to identify the most optimal sensor to implement in the design of the printed circuit board that will be within the metal structure of the grapple itself.



Figure 2: Three types of sensors

For the sensor to be as efficient as possible, it is desirable for the signal processing and conditioning to be done as close to the transducer as possible. Hence, integrating the electronic circuit is an advantage for this development.

To do the final design, four different tests are going to be carried out. The sensors will be under a temperature, mechanical, humidity and ageing test. The aim is to measure the response of the three kinds of sensors, choosing to use in the final prototype the one with the best response to mechanical stress while also considering the influence of temperature, humidity, and ageing. Ideally, it should not be influenced by those last three factors. The other option is for the sensor to have a linear or quadratic variation, function of those values, so it can be designed considering those variations.

Chapter 2. State of question

A first version of the grapple done by DERISYS based on the integration of an S-shaped sensor, like the one showed in Figure 3, presented a series of inconveniences according to:

- **Size:** this sensor may be larger than desired, as industrial settings might have a limited space, a bulky grapple might be less efficient and difficult to operate with. Screen printing allows for the customization of sensor (Figure 4) designed to fit specific shapes and sizes, which can be tailored to seamlessly integrate with the structural elements of the weighing grapple.
- **Mechanical interface:** doing the mechanical interface might be challenging, this is to say how well is the interaction between the sensor and the different mechanical components of the grapple. Issues may arise regarding alignment, stability, or the durability of the sensor's physical attachment to the grapple structure. As said before, screen printing allows designing the sensor to fit the grapple structure, also by easily integrating onto the metal structure of the weighing grapple, reducing the complexity of mechanical interface.
- **Weight:** despite it is a secondary criterion in this case, the additional weight of the sensor as well as the supporting electronics and mounting structures can impact the efficiency of the weighing grapple, for example, by limiting its maximum load capacity. However, the screen-printed sensor addresses this issue owing to its lightweight nature and compact size.



S TYPE PRESSURE SENSOR, PORTABLE S TYPE BEAM LOAD CELL SCALE SENSOR WEIGHING SENSOR 500KG FOR HOPPER WEIGHT HIGH PRESSURE TENSION WEIGHING, YANMIS

Figure 3: S-shaped sensor

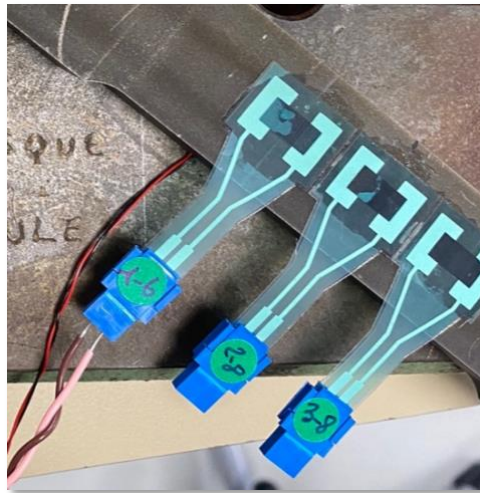


Figure 4: Three types of sensors used to measure stress

The most important criterion for the transducer (strain sensor) is to obtain an electrical reproducibility of the signal compatible with an industrial environment. This means that the realization of the transducer must guarantee a tolerance compatible with the calibration range determined or acceptable by the entire electronic circuit.

For this sensor to be as efficient as possible, it is desirable that the processing of the sensor signal and its conditioning are done at most near the transducer. This is why the integration of the electronic circuit is ideal for this development.

Chapter 3. Motivation

The engineering school of INSA Lyon in France hosts numerous research projects and collaborates with various companies in the sector. The large number of its laboratories gave me the idea to take advantage of my time at this school to carry out my Bachelor's thesis.

I then contacted the electrical department, which offered me the opportunity to work in collaboration with AEC Sérigraphie, a company within DERISYS that partners with INSA on various projects.

The project in question involved creating a weighing gripper using sensors made through screen printing, which caught my attention for several reasons:

- I was given the opportunity to visit the sensor manufacturing facility and gain firsthand insight into the fabrication processes, ranging from initial design phases to the coordination of various production processes (including screen printing, cutting, and performance testing) culminating in the final product.
- I wanted to learn more about screen printing, a technique I was unfamiliar with, which offers several advantages such as easy integration and low cost, as we will discuss later.
- I could develop the ability to make decisions based on experiment results and specifications. This includes selecting the sensor based on tests conducted for temperature, mechanical deformation, aging, and humidity drift. It also involves choosing the PCB design that ensures compliance with the specifications.

In a nutshell, the ability to make of a design according to the availability of components, in (this case the sensors), learn about the different stages involved in the making of a prototype, and efficiently respond to an everyday necessity, are the goals of every industrial engineer. This project seeks efficiency in an industrial environment, which is also a key point to learn in my training as an engineer.

Chapter 4. Project objectives

1. **Design a printed circuit board** according to the specifications given by DERISYS which are shown in Table 1.



<i>In French, direct specifications from DERISYS</i>	<i>Translation to English</i>
  <p>Spécifications fonctionnelles du dispositif</p> <ul style="list-style-type: none"> • Poids du grappin : environ 25kg Maxi en version 10T • Capacités : le grappin se déclinera en différentes capacités de charge, qui pourraient être 5T, 10T, 15T • Coefficient de sécurité mécanique : 2,5 fois la capacité nominale, résistance torsionnelle à définir • température de fonctionnement : -20°C, +50°C (attention au confinement du capteur) • résistance aux chocs : 5G ? à définir compte tenu des conditions d'utilisation. • Conception dans une démarche RSE, afin de garantir une durée de vie maximale du dispositif. • Alimentation électrique du grappin : batterie du type powerbank intégrée rechargeable depuis l'extérieur via un connecteur USB-B, potentiellement USB-C ultérieurement (pré-définition sur la carte électronique). • Tension d'entrée du circuit électronique souhaitée : 3,3V, donc capteur 3,3V • Liaison radio : technologie XBEE, 868MHz, réseau, avec antenne externe protégée. • Autonomie souhaitée : idéalement >100h d'utilisation, 50h mini • Interfaces de montage adaptables en fonction des marques, de types oreilles ou chapes • surface d'impression exploitable (capteur + électronique) : rectangle 80x130mm, hauteur connecteur Max : 10mm 	<p>Functional Specifications of the Device</p> <ul style="list-style-type: none"> - Weight of the grapple: approximately 25 kg max in the 10T version - Capacities: the grapple will be available in different load capacities, which could be 5T, 10T, 15T - Mechanical safety factor: 2.5 times the nominal capacity, torsional resistance to be defined - Operating temperature: -20°C to +50°C (note the sensor confinement) - Shock resistance: 5G? to be defined based on the conditions of use - Design with an RSE approach: to ensure maximum device lifespan - Power supply for the grapple: integrated powerbank-type battery, rechargeable from the outside via a USB-B connector, potentially USB-C later (pre-definition on the electronic board) - Desired input voltage for the electronic circuit: 3.3V, thus a 3.3V sensor - Radio link: XBEE technology, 868MHz, network, with protected external antenna - Desired autonomy: ideally >100 hours of use, minimum 50 hours - Adaptable mounting interfaces: depending on the brands, either ears or clevis types - Usable printing surface (sensor + electronics): rectangle 80x130mm, max connector height: 10mm

Table 1: Specifications of the design

- **Test different sensors** to select the most appropriate for my application, and then consider this results in the making of the PCB, to allow compatibility to the industrial exploitation.
- **Learn about the different stages** of an industrial project, from an initial problem that needs to be addressed (the inefficiency of sensor type S in measuring weight), to the final design of a sensor that fits better in an industrial setting, to its implementation in the circuit design of a weighing grapple.
- **Prove the advantages of printed electronics**, like its effectiveness and efficiency in the industrial exploitation.

- **Understand all the parts involved in doing a real engineering project** like this, where enterprises like AEC, within of DERISYS, work with INSA laboratories to carry out an industrial project.
- **Design a prototype that improves the industrial performance**, in this case the weighing grapple.

Chapter 5. Alignment with the Sustainable Development Goals (SDG)

Number 9: Industrial, innovation and infrastructure.

This project is to improve and resolve issues that we encounter in the industry today. Applying printed electronics in this case may lead to have printed electronics in other applications, so it contributes to technological development.

Chapter 6. Work methodology

The working plan of the project is the following:

Week 1. Thermal drift of sensor

- Measuring resistance function of temperature
- Range of temperature -20°C to 60°C
- Analyse the respond plotting resistance function of temperature

Week 2. Mechanical sensitivity of sensor

- Instrumentation of device using classical strain gauge
- Measuring R function of strain
- Analyse the respond of the sensor

Week 3. Humidity drift

- Measuring resistance function of humidity
- At 80% relative humidity, for 2 days
- Analyse the drift respond of the sensor

Week 4. Thermal ageing

- Static ageing: 24H at 80°C, 48H at 80°C
- From -20°C to 80°C at a rate of 1°C/min stopping every 10°C for 10 min
- Measuring R function of time
- Analyse the respond of the sensor due to thermal ageing.

Week 5 and Week 6. Proposition of sensor network linked to application requirements.

- Testing the different designs
- Analyse the respond of the sensor.

Working plan

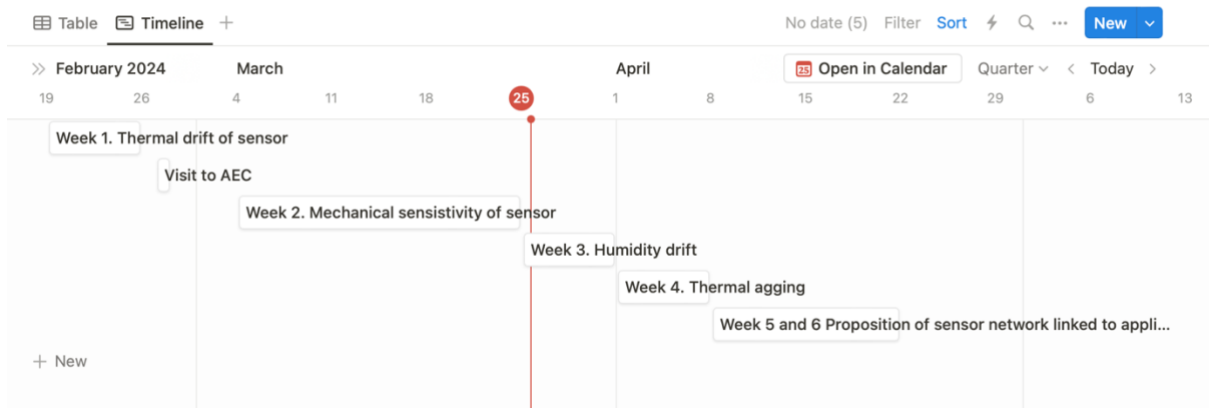


Figure 5: Gantt diagram of the working plan

Chapter 7. Resources

In this project, fortunately, a large variety of resources have been at my disposal. In the first place, the sensors were fabricated with AEC sérigraphie technology at its laboratories. A considerable amount array of machinery was used in the different stages of the fabrication process, from screen printing machines to laser tools used to cut the wanted shapes of the sensors. I also had the opportunity of visiting the factory where they were produced, along with observing their manufacturing process, topic on which I will elaborate in the forthcoming AEC Sérigraphie section.

Secondly, the laboratories of INSA provided the equipment to do the testing of the sensors. Including an oven for the temperature test, a temperature humidity test chamber for the thermal ageing and humidity experiments (Figure 6) and a material testing machine for the mechanical strain tests (Figure 7). Also, the necessary tools like the samples and commercial sensors used in the strain tests.

To obtain all signal data from the sensor testing, it was imperative to utilize the DEWE (Figure 8), a data acquisition technology developed by Dewesoft. A company which also generated the software that processed the data obtained of the sensors, which had the same name, Dewesoft.

Once the characterizations of the sensors were done, ALTIUM was the software adopted to propose the design of the electronic interface schematic and of final printed circuit board (PCB).

For a better insight of this types of machines and software, a detailed explanation is to continue:

Temperature humidity test chamber

This machine is developed by Weiss Technik to provide a controlled environment where precise temperature and humidity conditions need to be maintained to simulate the real-world scenarios where our sensor is going to be under.

This type of equipment is going to be used in the temperature, thermal ageing, and humidity test. The samples are placed inside the chamber after the calibration to ensure the accuracy of the measurements. A configuration with the specifications is made before, directly on the screen on the front of the machine, which is implemented by its control system.



TEMPERATURE TEST CHAMBERS, TYPE TEMPEVENT, WEISS TECHNIK

Figure 6: Humidity temperature chamber.

Mechanical stress machine

The mechanical stress machine developed by SHIMADZU, is an advanced equipment used for testing the mechanical properties of materials. It applies controlled stress to samples to measure properties like tensile strength, elasticity, and deformation behaviour, the last one being our case. It offers precise measurement capabilities and can simulate various real-world conditions to assess how the sensors will respond under stress.

The software used to control the machine is TRAPEZIUM X, developed by SHIMADZU, where we will do the configuration for the mechanical strain test, which is specifications will be displayed in this test section.



SHIMADZU, AUTOGRAPH AGS-X SERIES

Figure 7: Mechanical stress testing machine

DEWE

The specific name of the device developed by Dewesoft is SIRIUS-UNI Universal. This is a data acquisition gadget, equipped with multiple channel configurations, capable of measuring with high precision strain gauges, bridge sensors and voltage.

This technology can provide with high dynamic range and low noise. It also uses DualCoreADC technology, developed also by Dewesoft, used to precisely convert signal analogic inputs analogic to digital outputs with minimum noise. In our application, this system is going to be used to acquire the signal received from the sensors throughout the tests.

The type of configuration is going to be done by the Dewesoft software. For each test, an appropriate one has been fixed, specified in each test section.

The data treated in Dewesoft will be transformed to a .mat file that is later going to be managed by MatLab, to generate the charts used to characterise the sensors.



SIRIUSi-8xUNI data acquisition system with universal signal inputs

Figure 8: DEWE

ALTIUM

This software platform is primarily used, as in our case, for designing electronic circuit boards. It offers tools for schematic capture, component placement, and routing, facilitating the creation of complex multi-layer PCBs. The software includes component libraries and supports circuit simulation for verifying design functionality.

Its capacity and ease of use make this software ideal to design a final PCB, that responds adequately to the demands of the project.

Chapter 8. Fabrication and characteristics of sensors

8.1. AEC sérigraphie

As mentioned at the introduction, INSA Lyon works in partnership with AEC sérigraphie in various projects, including the production of the sensors under testing. Therefore, I was given an opportunity to visit the factory where the sensors were fabricated to learn about how these types of projects are carried out in an enterprise. The production chain consisted in various steps, each done by an employee or team of employees, who kindly explained to me how everything worked. The factory is located in Régný, a small town near Lyon.

1. Design

A person implements the previously designed sensor in the software unic.Draw. Each layer is set up in the software, in this stage it could happen that small changes are done in order to improve the functionality of the design. Next step is to flash print the design on a film that will be used later as the pattern for screen printing.

2. Sensor planification

Afterwards, the planification of the different stages to produce the sensor is carried out. This is done considering aspects like working hours, time of production and materials supply, for then to calculate total time of production and total cost.

3. Fabrication process

a) Preparation of the screen printing.

The substrate and screen (that can be metallic or polymerous) is ordered and supplied. In the case of the substrate, it is needed to be cut and tested to ensure that it withstands the subsequent processes (for example the oven at 130°)

Regarding the screen, we need its mesh parameter to be small for precision, but not too small that it doesn't allow, in this case the silver ink, to pass through the material. A cleaning of the screen beforehand and between layer deposition is also needed.

b) Screen printing process.

Screen printing for the development of the sensor is a process that involves depositing conductive materials, such as silver inks, onto a substrate using a mesh and a stencil. The sensor design is created on the stencil, and the ink is pressed through the mesh to transfer the pattern onto the substrate. This method enables the production of precise and reproducible sensors in large quantities in a cost-effective manner. The steps to follow are shown in Figure 9 and are:

1. Deposition of a photoUV mask on the substrate.
2. Placing the film with the design made in negative (done in step 1).
3. Applying UV radiation that only affects the part not covered by the design.
4. Cleaning of the UV mask that was not affected by the UV radiation with a dissolvent (the activated UV mask won't be affected by the cleaning of the material layer)
5. Deposition of the ink that is then pressed through the mess onto the substrate. We can see in Figure 10 the ink being deposited controlled by a squeegee, the metallic blade shown. In the case if the sensor, two inks are used: silver and carbon.
6. Each deposition layer is exposed to high temperatures in a in a thermal tunnel for the product to be then placed afterwards, in an oven at 130°.
7. Additionally, we can clean the photoUV mask so we can use the screen again.

c) Adding of a layer to protect the design (part in green)

d) Laser cutting with the desired shape of the sensor.

e) Lastly, the sensor is tested to verify the sensor proper functioning.

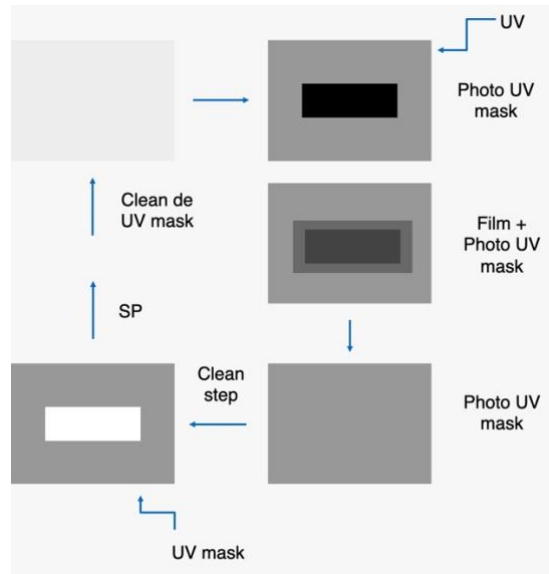


Figure 9: Steps for screen printing



Figure 10: screen printing using silver ink

8.2. Screen printing

Screen printing is an ancient technique dated in the 3000 b.C in the Fiyi islands, which it just consisted in using leaves with holes in them where the ink was distributed. Nowadays, the principle is the same, where a mesh stretched over a frame is used to transfer ink onto a surface, except in areas blocked by a substance impermeable to ink. This creates a design on the desired surface.

This idea is then used in electronics, to be able to successfully print electronic circuits on substrates such as PCBs or sensors. It uses a special mesh or stencil to transfer conductive or insulating ink onto the substrate. This method allows for the creation of precise patterns of electrical conductors that connect components such as resistors, transistors and microchips in electronic devices. It is essential for the efficient and accurate manufacturing of modern electronic equipment, and the technology developed by Arc en Ciel.

8.3. Sensors addressed

Three sensors are obtained with the following characteristics:

Sensor 1: D24-002 GRAPIN / Ag ECI 1014 / Carbone ECI 8120

Sensor 2: D24-001 Jauge / Ag ECI 1014 / Carbone ECI 8001

Sensor 3: D24-001 Jauge / Ag ECI 1014 / Carbone ECI 7004 30%, ECI 7002 70%

A design of the sensor has been done in Figure 11, that shows the structure of the sensor, made by carbon and silver inks.

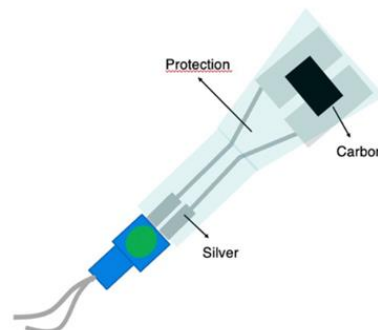


Figure 11: screen printed sensor

The carbon of the sensors is piezoresistive, which means that the resistivity of the material varies depending on the mechanical stress. The sensor will change its resistance in proportion to the stress in a specific direction.

It has been mentioned before in the resources section, that a commercial sensor is used in the mechanical test. One might ask why this sensor is not used in our application, the weighing grapple. The reason is that this sensor has a low resistance which results in more power consumption, reducing the autonomy of the device, that needs pouring provided by batteries.

With bigger resistances, like the ones of the sensors of $5k\Omega$ and more, we will have low-battery consumption. On the contrary, the sensors may suffer from a bigger thermal and humidity drift, which will be analyzed in future sections.

Chapter 9. Test results

9.1. Temperature

The first test done was measuring the resistance according to temperature. The experiment consisted in placing the sensors inside the oven that was configured to vary the temperature from -20°C to 55°C , by a rate of 2°C per minute in order to have a homogenous temperature in the whole oven.

Using a DEWE, we measured the resistance of the three sensors, using two samples of each to ensure the reliability of the results. The first digit (1, 2 or 3) corresponds to the type of sensor and the second digit is the number identifying which sample has been used of each type. We obtained the data in the tables below. Each data corresponds to two cycles of temperature.

Sensor 1

Type 1.1.	R _{-20°C} (Ohm)	R _{55°C} (Ohm)	Linear fit	Quadratic
Data 1	5184	7162	$24.73x+5505$	$0.2032x^2+16.41x+5464$
Data 2	5273	7085	$23.9x+5539$	$0.1979x^2+15.67x+5506$
Data 3	5373	7031	$21.57x+5644$	$0.1691x^2+14.66x+5611$
Data 4	5472	7058	$20.48x+5734$	$0.1549x^2+14.09x+5703$
Data 5	5428	7016	$19.89x+5721$	$0.1485x^2+14.02x+5683$

Table 2: Resistance results for the sensor sample 1.1.

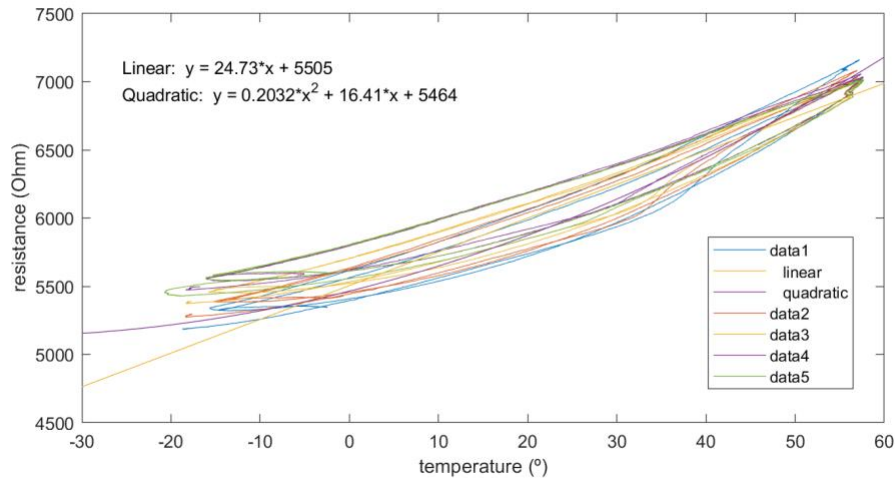


Figure 12: Resistance according to temperature of sensor sample 1.1.

Type 1.2.	R _{-20°C} (Ohm)	R _{55°C} (Ohm)	Linear fit	Quadratic
Data 1	4855	6741	22.52x+5262	0.1599x ² +15.97x+5230
Data 2	5171	6786	21.12x+5433	0.1628x ² +14.36+5406
Data 3	5389	6820	18.91x+5617	0.1383x ² +13.26x+5589
Data 4	5513	6882	18.03x+5730	0.1267x ² +12.8x+5705
Data 5	5439	6810	17.34x+5706	0.1143x ² +12.82x+5676

Table 3: Resistance results for the sensor sample 1.2.

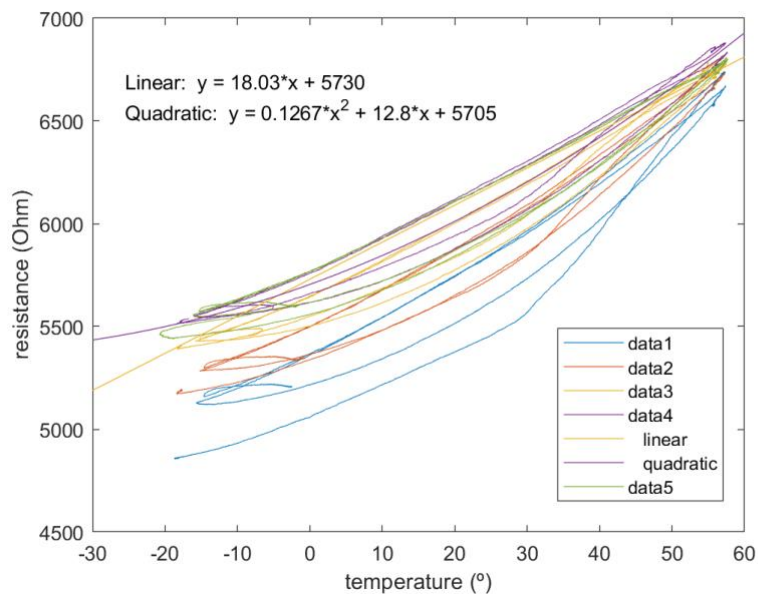


Figure 13: Resistance according to temperature of sensor sample 1.2.

$$\Delta R = R_{55^{\circ}\text{C}} - R_{-22^{\circ}\text{C}}$$

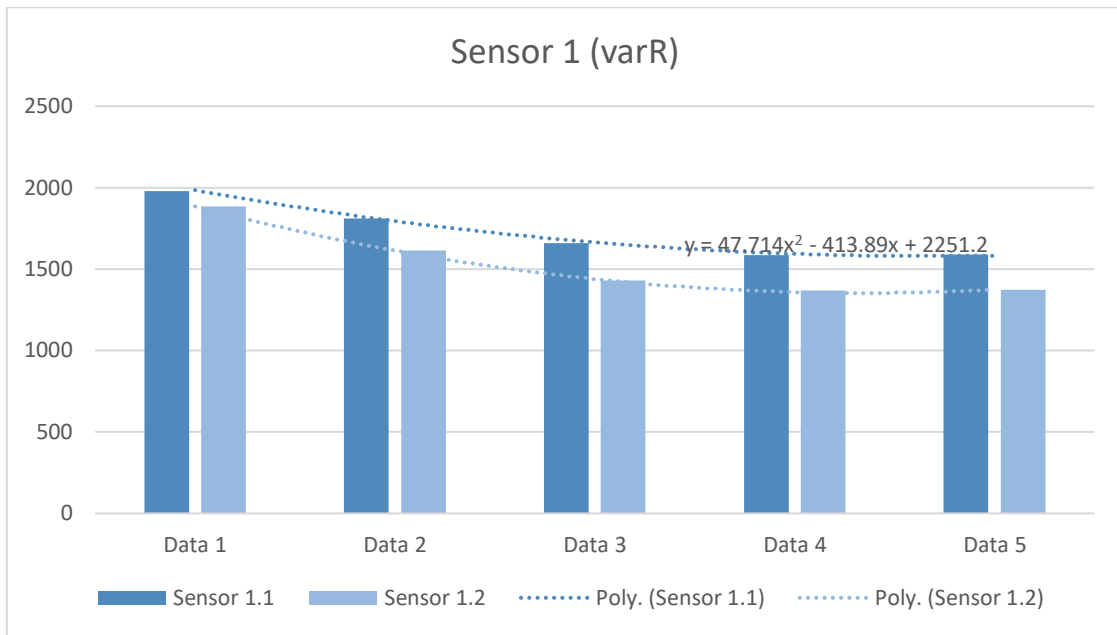


Figure 14: chart of ΔR of sensor 1

$$y = ax + b; \text{ value of } a$$

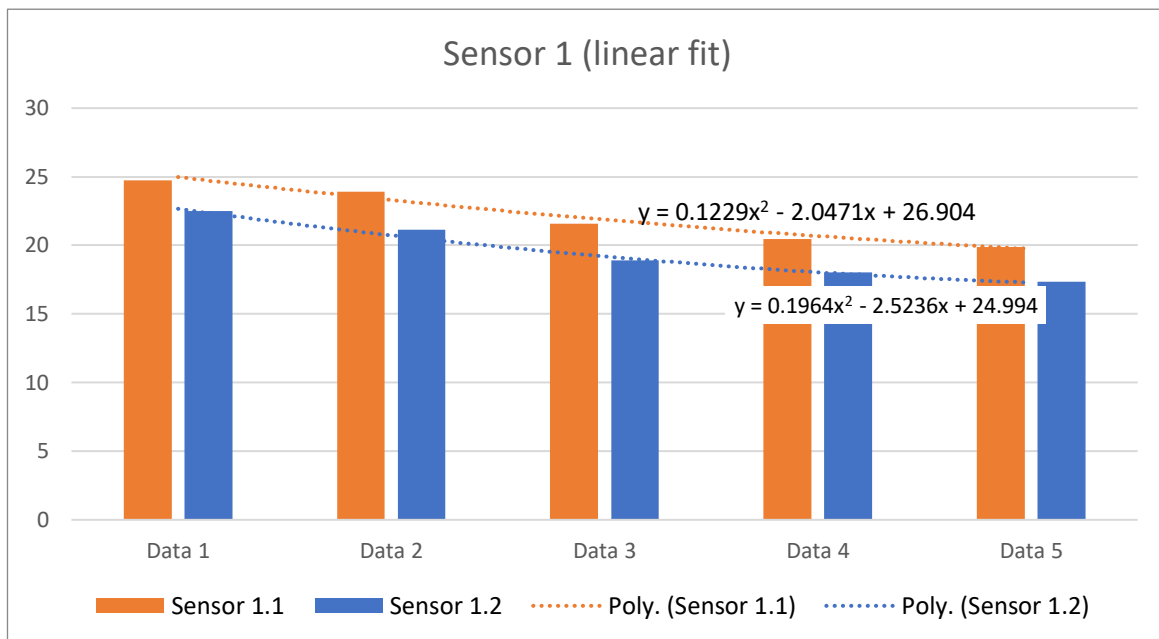


Figure 15: value a of linear fit

Analysis:

In the case of sensor 1, we can see a quadratic tendency on the value of resistance depending on the temperature, which means there is an aging of the sensor, which causes the measure to

be lower and lower as well as the difference of the resistance to the higher temperature (55°C) and the lowest (-22°C) indicating fatigue of the material.

According to the results, the aim would be to see if this tendency stops, and the sensor measurement stabilises, which can be seen in the future thermal ageing test.

Sensor 2

Type 2.4.	R _{-20°C} (Ohm)	R _{55°C} (Ohm)	Linear fit	Quadratic
Data 1	3637	7387	42.66x+4004	0.6539x ² +15.89x+3873
Data 2	3415	6317	36.47x+3645	0.5397x ² +14.05x+3356
Data 3	3202	5703	31.24x+3452	0.4467x ² +12.99x+3363
Data 4	3080	5408	28.92x+3319	0.4082x ² +12.06x+3238
Data 5	2988	5233	26.99x+3261	0.3752x ² +12.17x+3164

Table 4: Resistance results for the sensor sample 2.4

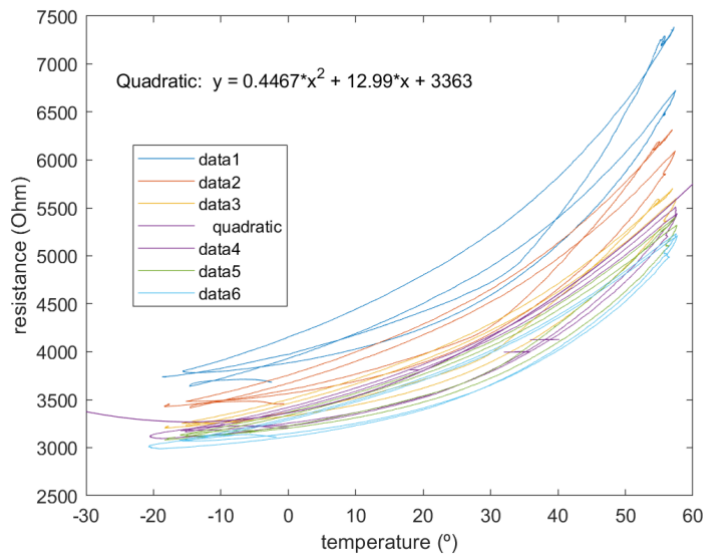


Figure 16: Resistance according to temperature of sensor sample 2.4.

Type 2.5	R _{-20°C} (Ohm)	R _{55°C} (Ohm)	Linear fit	Quadratic
Data 1	3851	7881	45.33x+4245	0.6876x ² +17.18x+4107
Data 2	3578	6554	37.22x+3818	0.5395x ² +14.81x+3729

Data 3	3327	5849	$31.44x+3588$	$0.4385x^2+13.52x+3501$
Data 4	3190	5524	$28.96x+3390.396$	$2x^2+12.6x+3360$
Data 5	3094	5338	$26.97x+3375$	$0.3638x^2+12.6x+3281$

Table 5: Resistance results for the sensor 2.5.

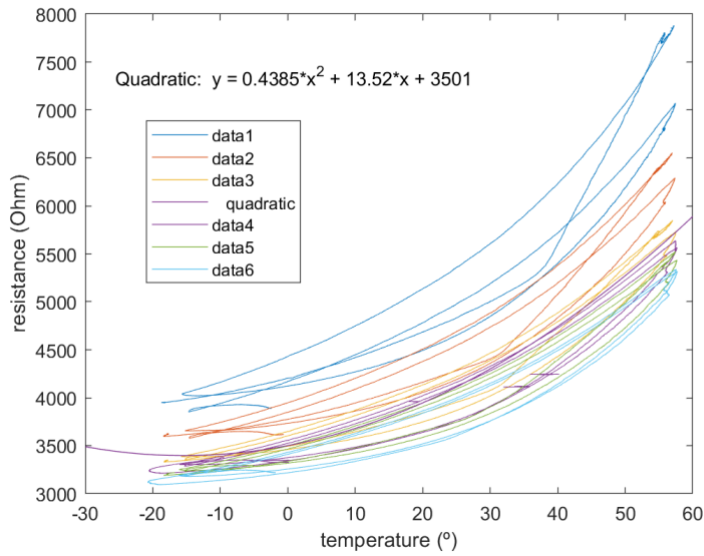


Figure 17: Resistance according to temperature of sensor 2.5.

$$\Delta R = R_{55^{\circ}\text{C}} - R_{-22^{\circ}\text{C}}$$

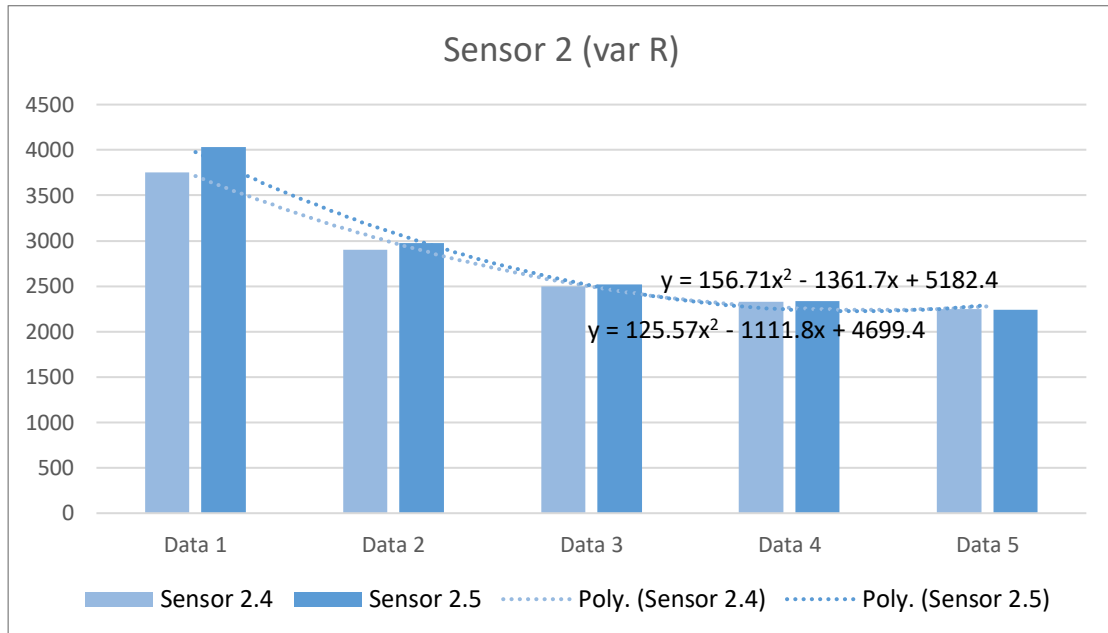


Figure 18: chart of ΔR of sensor 2

$$y = ax^2 + bx + c; \text{ value of } a$$

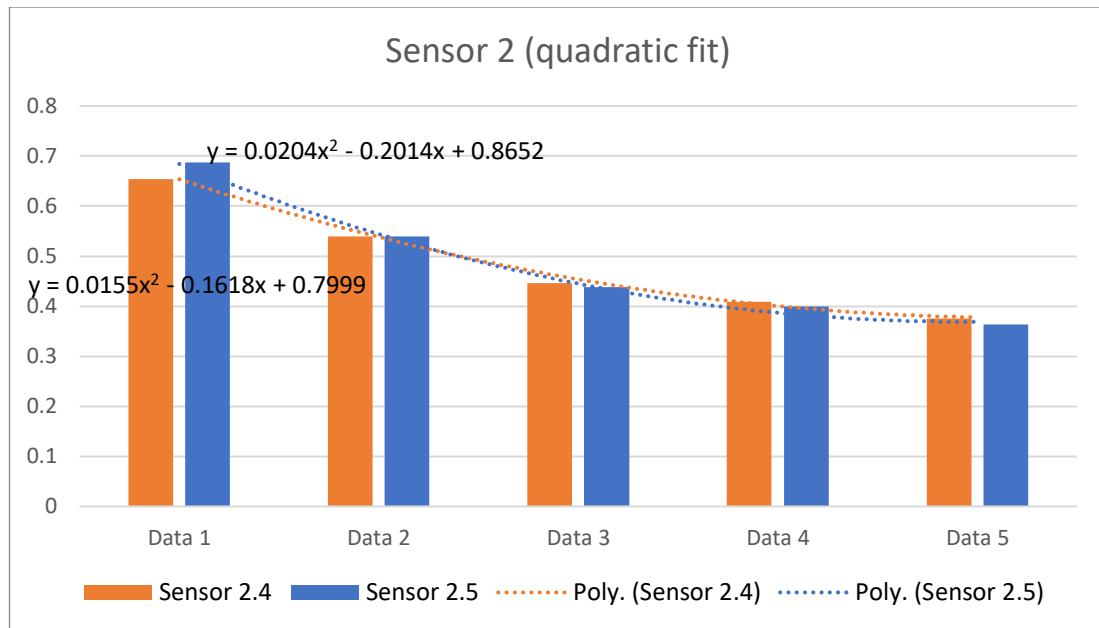


Figure 19: value a of quadratic fitting

Analysis:

In this case, since the decrease of the sensor resistance is quadratic, an analysis of the most significant component of the fitting (value of a) is the most appropriate to review. Like with sensor 1; sensor 2 shows a fatigue, which causes a decrease in its resistance as well as in the gap between highest and lowest temperature resistances.

Sensor 3

Type 3.1.	R _{-20°C} (Ohm)	R _{55°C} (Ohm)	Linear fit	Quadratic
Data 2	1.114e4	1.152e4	-1.065x+1.129e4	0.0668x ² -3.84x+1.128e4
Data 3	1.113e4	1.165e4	-2.236x+1.136e4	0.07628x ² -5.353e4
Data 4	1.111e4	1.161e4	-2.171x+1.133e4	0.06021x ² -4.657x+1.132e4
Data 5	1.108e4	1.127e4	-1.014x+1.12e4	0.03064x ² -2.224x+1.119e4

Table 6: Resistance results for the sensor 3.1.

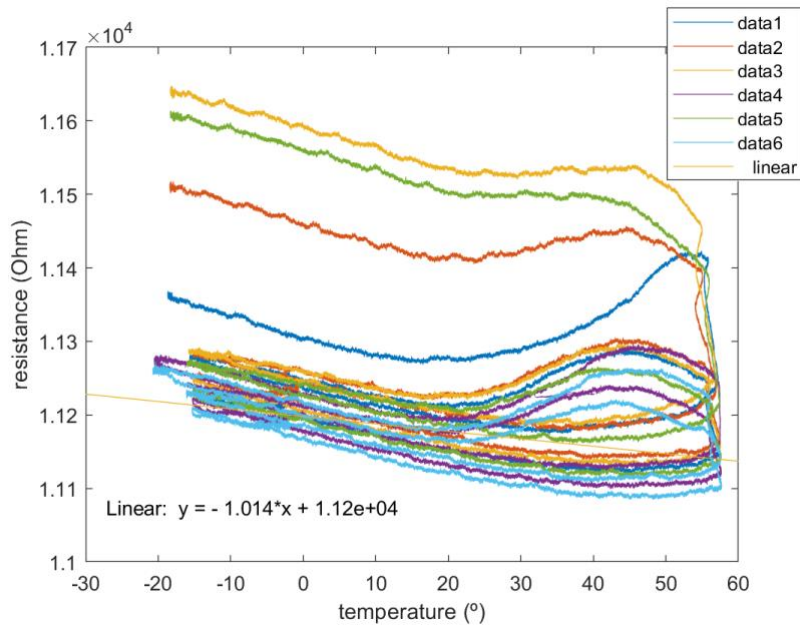


Figure 20: Resistance according to temperature of sensor 3.1.

Type 3.5.	R _{-20°C} (Ohm)	R _{55°C} (Ohm)	Linear fit	Quadratic
Data 2	1.262e4	1.303e4	-0.9601x+1.278e4	0.07696x ² -4.157x+1.277e4
Data 3	1.262e4	1.319e4	-2.232x+1.287e4	0.08927x ² -5.879x+1.285e4
Data 4	1.26e4	1.315e4	-2.187x+1.283e4	0.07049x ² -5.097x+1.282e4
Data 5	1.255e4	1.276e4	-0.8912x+1.267e4	0.03526x ² -2.284x+1.266e4

Table 7: Resistance results for the sensor 3.5.

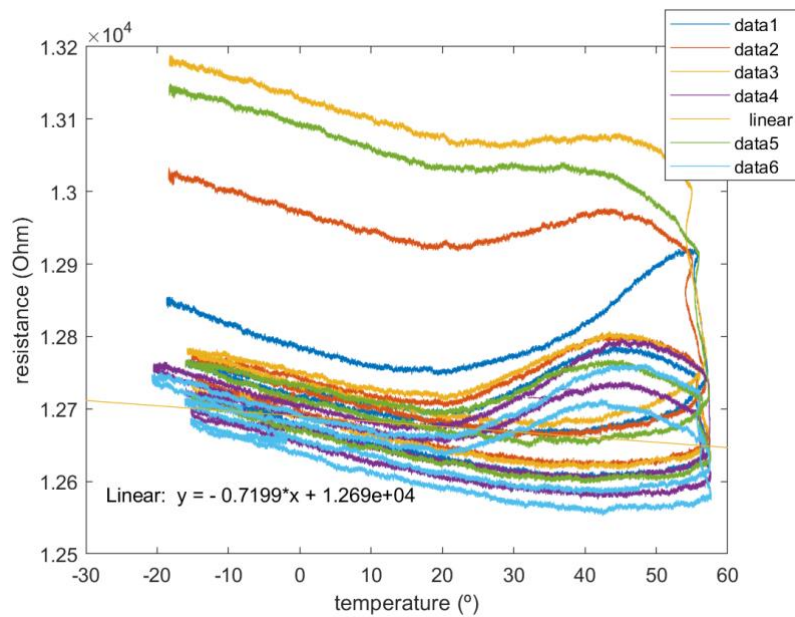


Figure 21: Resistance according to temperature of sensor 3.5.

$$\Delta R = R_{55^{\circ}\text{C}} - R_{-22^{\circ}\text{C}}$$

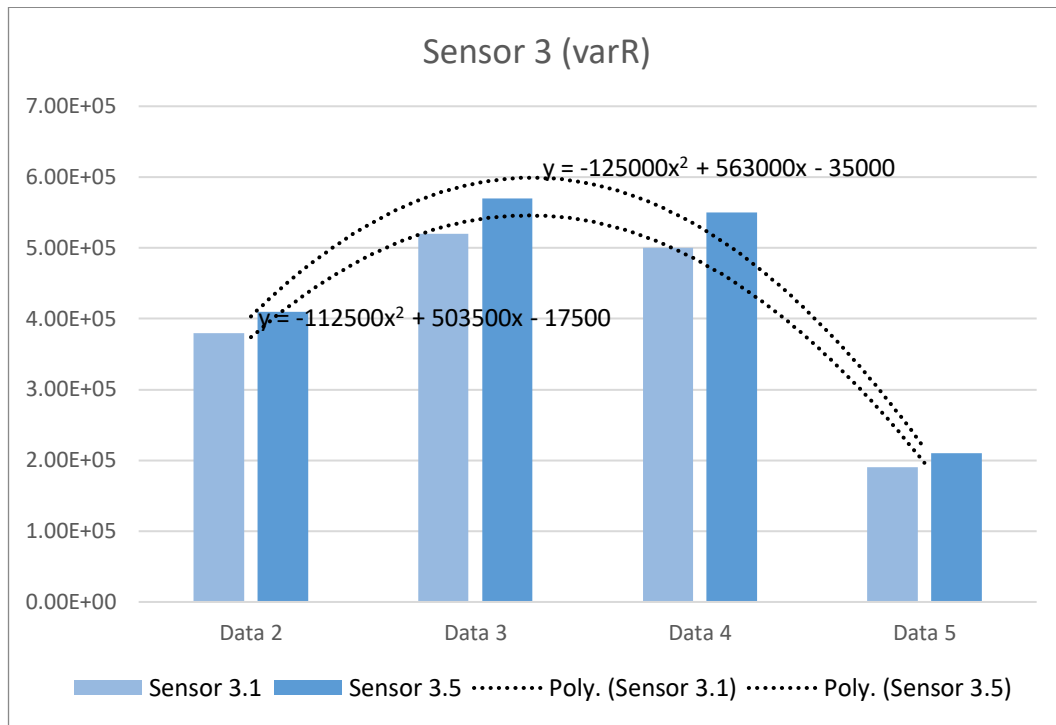


Figure 22: chart of ΔR of sensor 1

$y = ax + b$; value of a

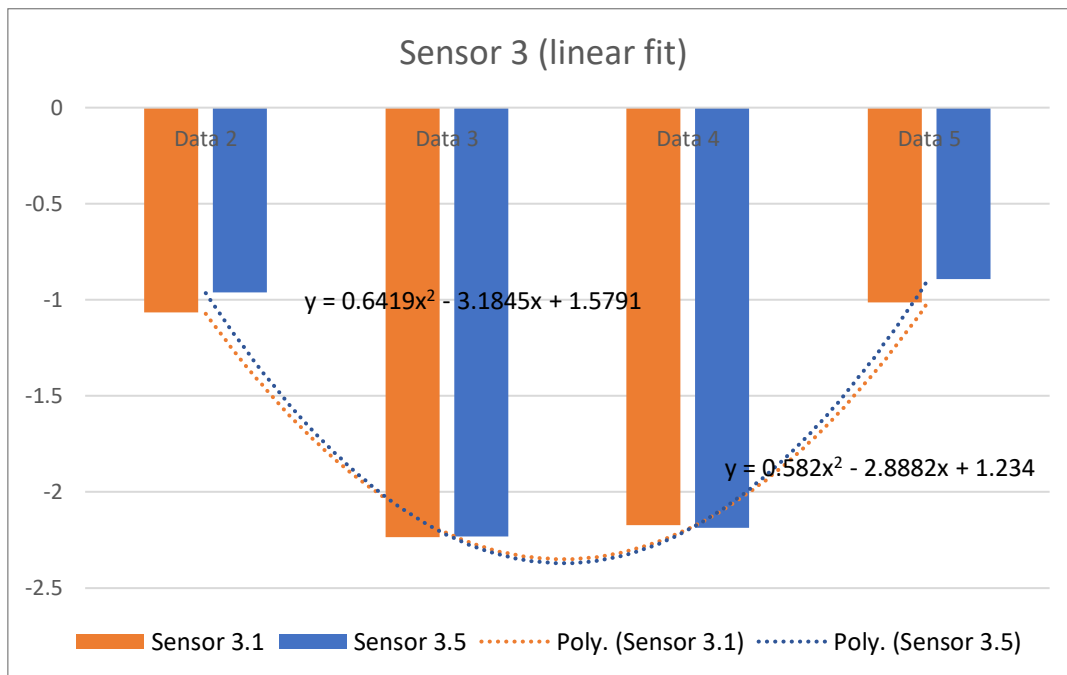


Figure 23: value a of linear fitting

Analysis:

In this case, the results greatly differ from sensor 1 and 2, where the tendencies are similar to that of a parabola, the results show little variation of the resistance, which may indicate an indifference of sensor 3 regarding temperature.

Conclusion

It is important to point out that in sensor 1, the differences between resistances ($\Delta R = R_{55^{\circ}\text{C}} - R_{-22^{\circ}\text{C}}$) as well as the variation between a values is quite high if we compare them to values in sensor 3, which also has a linear fitting. This means that sensor 3, as we predicted, is not really affected by temperature varying. It seems that in the case of choosing sensor 1 or 2, a compensation of temperature will be needed in the making of the PCB design, whereas if we choose sensor 3, temperature drift can be negligible.

Another point to consider is that the two sensors of each type share the same tendency, so it is not necessary to do more tests with other examples of the same sensor.

Finally, it can be pointed out, that it is normal to have a first expansion stage when measurement starts, for it to then stabilise and have a more linear behaviour.

9.2. Mechanical strain

The mechanical strain test is crucial to know how the resistivity of the sensors responds to mechanical stress, so we can choose the best one to do our circuit.

Preparation

In this experiment both the mechanical strain machine (Figure 24) to perform the mechanical strain of a still sample (which is the same material as the future gripple) and the DEWE to quantify the stress were used. Moreover, a commercial sensor (with a gauge factor of 2) was used as a way of calibration, measuring the strain of the sample regarding time. It is used to

compare with the measures of the other three sensors, whose design is supposed to provide a better, more precise measurement.

As we can see in Figure 25, we apply glue to place the commercial sensor in one of the sides. After this, we use a welder and tin to make the contacts between the sensor and the cables red and black for then to protect all by a layer of silicon. On the other side we may set the sensors by sticking them with the adhesive. Nevertheless, we ended up using also glue to place the sensor, as the adhesive did not stick well, which interfered with the precision of measures.

In this case, sensors of same the same type are being used. On the other hand, the commercial sensor was used as a reference for the charts, having in axis y the resistance of the strain sensors and in axis x the strain measured by the commercial. Three tests of 10 cycles each were done.

The mechanical strain machine was configurated by TRAPEZIUM X software the abiding by the following conditions:

Characteristics of the sample:

- $L=180\text{mm}$
- $Le=144,7\text{mm}$
- $e=0,6\text{mm}$
- $w=25\text{mm}$

Characteristics of the tensile-testing machine:

- We know that the maximum deformation in application is $174 \mu\text{def}$.
- I imposed a maximum deformation of 0.3 mm on the specimen to cover the entire deformation range.

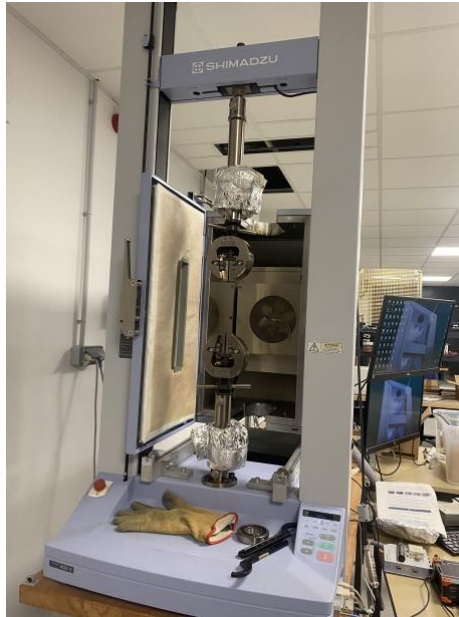


Figure 24: mechanical strain machine

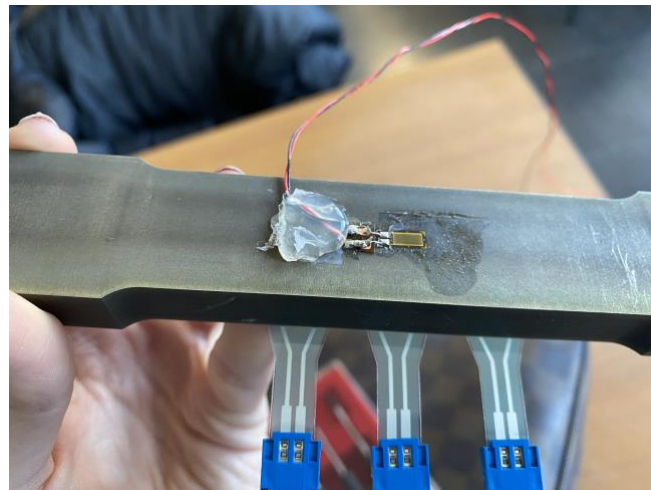


Figure 25: placement of the comercial sensor

Results

As mentioned earlier, it is important to determine how different carbon inks respond to deformation. This is achieved by determining the gauge factor, which indicates the resistance variation relative to deformation. In our case, the commercial sensor has a gauge factor of 2, and we are interested in achieving a deformation gauge factor of at least 1.5 for our sensor.

We may take a closer look at the Gauge factor:

$$GF = \frac{\Delta R/R}{\Delta L/L}$$

R → initial resistance

L → initial length

ΔR → change in resistance

ΔL → change in length

Initially, a quarter bridge configuration of the DEWE was made and the following results were obtained:

<i>Type 1</i>	<i>Linear fit</i>	<i>Gauge factor</i>
Test 1	0.006912x+1.334e4	0.006912
Test 2	0.004648x+1.334e4	0.004648
<i>Type 2</i>	<i>Linear fit</i>	<i>Gauge factor</i>
Test 1	-0.01301x+1.672e4	0.01301
Test 2	3.647x-6321	3.647
<i>Type 3</i>	<i>Linear fit</i>	<i>Gauge factor</i>
Test 1	0.01197x+6373	0.01197
Test 2	0.01772x+6325	0.01772

Table 8: Mechanical strain tests 1 and 2

Analysis:

The results are not satisfactory, the GF is too low (we wanted at least 1.5) and the linear fit is not good in any of the sensors, we could see that the results have a lot of noise due to the output not being attenuated, but apart from that, the change in the resistance was not enough to provide a good measurement.

There are a few reasons why a quarter bridge configuration does not work. Firstly, the sensitivity of the carbon is low, this means that the exit signal is too low for the DEWE to amplify to detect the small variances in the strain. Secondly, the DEWE is consuming too much power in a quarter bridge configuration, as it needs to excite the Wheatstone bridge.

The solution was to change the configuration of the DEWE to have a better quality of the response, using a **full Wheatstone bridge configuration** instead of a quarter bridge one:

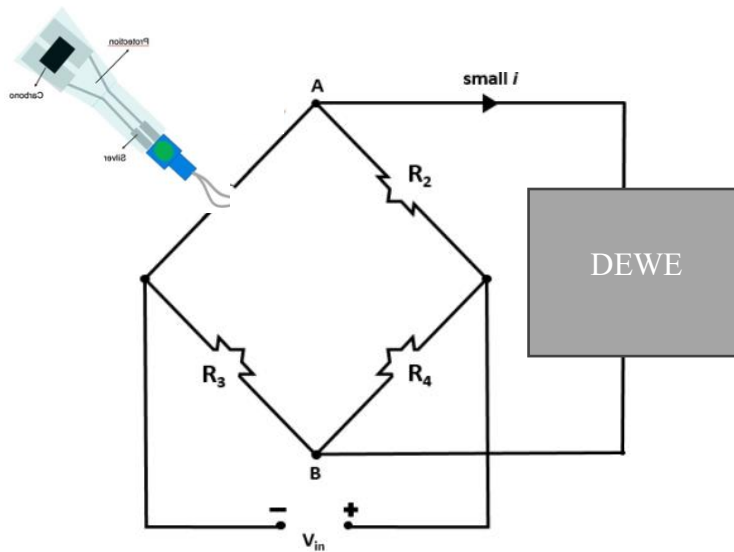


Figure 26: configuration of the DEWE

This type of configuration is used to measure low resistances. When there is no current in the galvanometer (V_{in}), we know that the system is balanced and we can measure R_s , which is the resistance of the sensor.

The DEWE had this configuration (with the resistances) inside, but in this case, we do the an external Wheatstone bridge, so we can choose the resistances to better match the initial

resistance of the sensors. This helps the DEWE to measure the low variation of the sensor resistance.

The GF is then calculated from the measurement of the variation of voltage:

$$\Delta V_{out} = \frac{(R_s + \Delta R_s) \cdot R_4 - R_2 \cdot R_3}{((R_s + \Delta R_s) + R_2) \cdot (R_3 + R_4)} \cdot V_{in} \quad [Eq1]$$

Because $R_2 = R_3 = R_4 = R$ and $\frac{R_s}{R_2} = \frac{R_3}{R_4}$, we obtain:

$$\frac{\Delta V_{out}}{V_{in}} = \frac{\Delta R_s}{4R}; \quad [Eq2]$$

$$GF = \frac{\Delta R_s / R_0}{\Delta L / L_0} = \frac{(4R \cdot \frac{\Delta V_{out}}{V_{in}}) / R_0}{\Delta L / L_0} = \frac{4R}{R_0} \cdot \frac{\Delta V_{out} / V_{in}}{\Delta L / L_0} \quad [Eq 3]$$

Sensor 1

Temperature test results of sensor 1 are:

<i>Sensor 1</i>	<i>Linear fit</i>	<i>Gauge factor</i>
Test 3	-0.0005373x+18.91	2.26

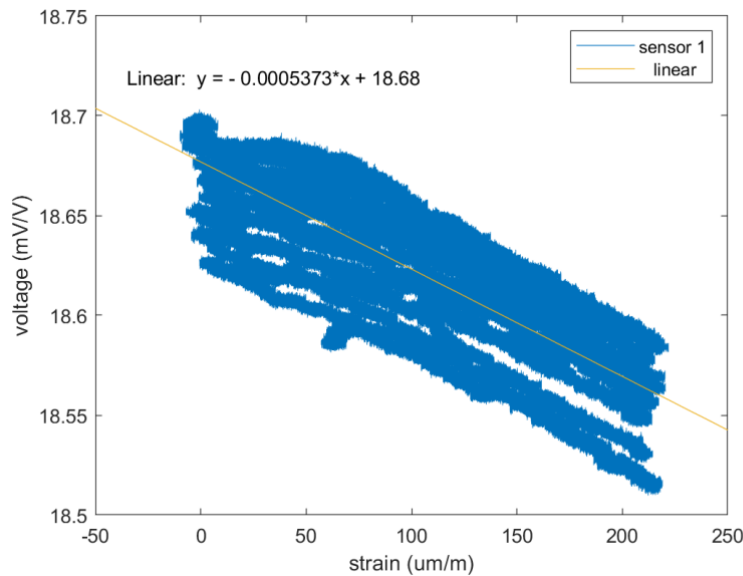


Figure 27: Voltage variation function of strain of sensor 1

We calculate the gauge factor taking into account that the linear fitting gives the value of mV/V per $\mu\text{m}/\text{m}$, using Eq3:

$$GF^1 = \frac{\Delta R_S/R_0}{\Delta L/L_0} = \frac{4R}{R_0} \cdot \frac{\Delta V_{out}/V_{in}}{\Delta L/L_0} = \frac{4 \cdot 5600}{5330} \cdot 0.0005373 \cdot 10^3 = 2.26$$

We compare, regarding time, the strain of the commercial and the varying of the voltage of the sensor 1:

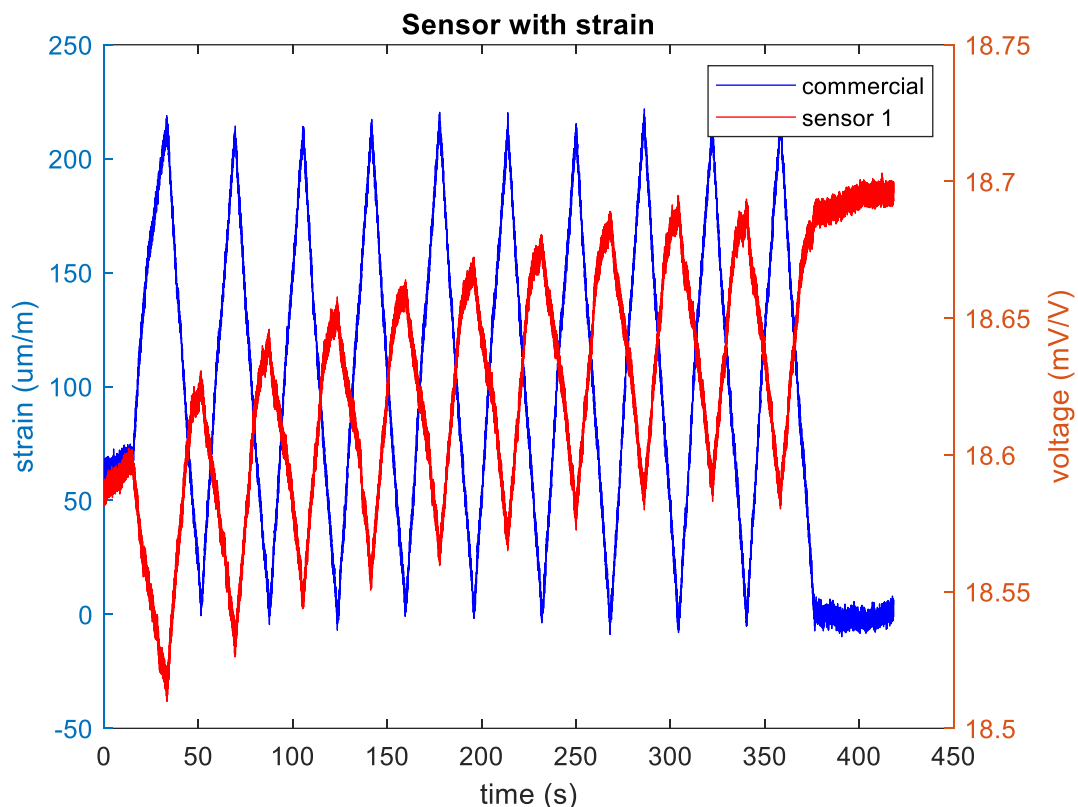


Figure 28: Resistance function of time and strain function of time

Analysis:

A gauge factor value of 2.26 is highly satisfactory for our application, as it is similar to those of the metal gauges, making sensor 1 a strong candidate for our needs. Additionally, we observe that the resistance is inversely proportional to the deformation measured by the commercial sensor, allowing us to determine the material deformation and subsequently calculate its

¹ The 10^3 component is due to the units of a $\mu\text{m}/\text{m}$ and mV/V

weight. Furthermore, the resistance shows a slight tendency to increase but stabilizes progressively with each cycle.

Sensor 2

Temperature test results of sensor 2 are:

<i>Sensor 2</i>	<i>Linear fit</i>	<i>Gauge factor</i>
Test 3	-0,0001779x-2,747	0,71

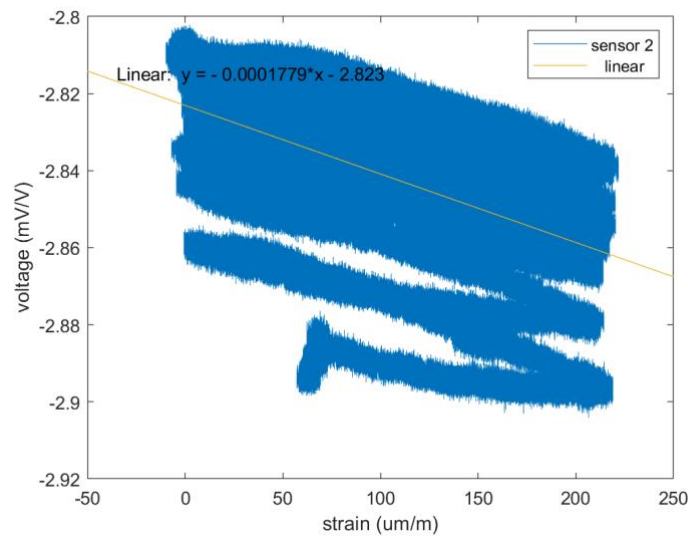


Figure 29: Voltage variation function of strain of sensor 2

The same calculus is done for sensor 2:

$$GF = \frac{\Delta R_s / R_0}{\Delta L / L_0} = \frac{4R}{R_0} \cdot \frac{\Delta V_{out} / V_{in}}{\Delta L / L_0} = \frac{4 \cdot 15900}{15880} \cdot 0.0001779 \cdot 10^3 = 0.71$$

We also compare the commercial and sensor 2 regarding time:

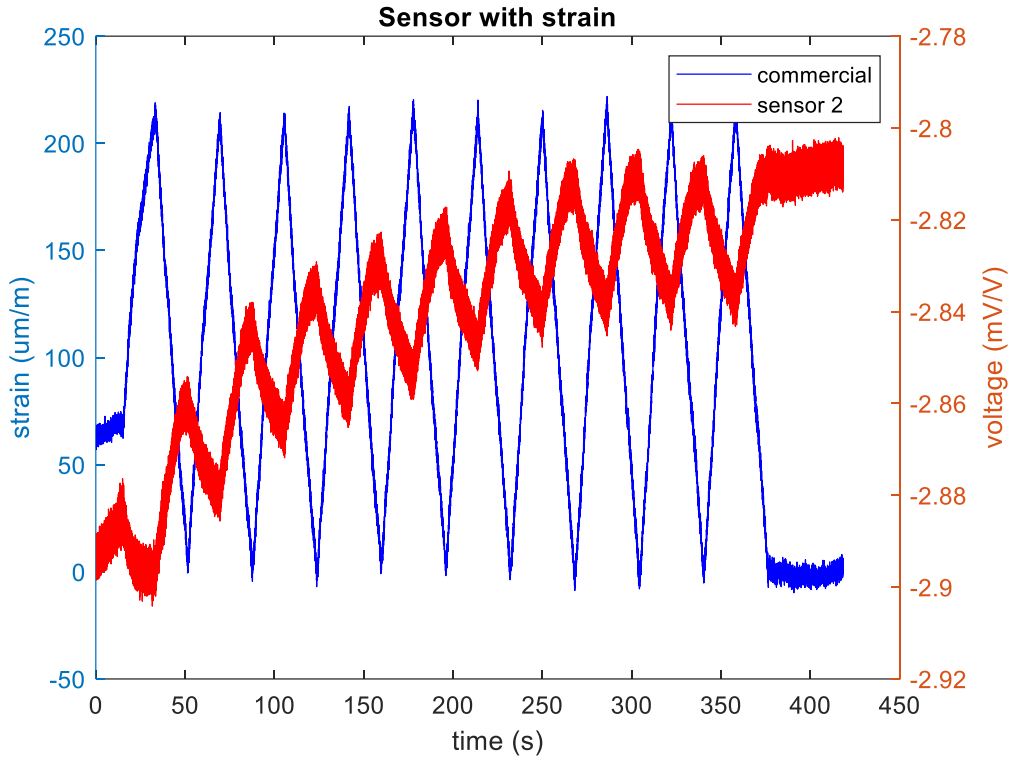


Figure 30: Resistance function of time and strain function of time

Analysis:

Unfortunately, a gauge factor of 0.71 is not enough, as we can see in Figure 30, so we must dismiss sensor 2.

Sensor 3

Temperature test results of sensor 3 are:

<i>Sensor 3</i>	<i>Linear fit</i>	<i>Gauge factor</i>
Test 3	0,0007568x-6,637	3.09

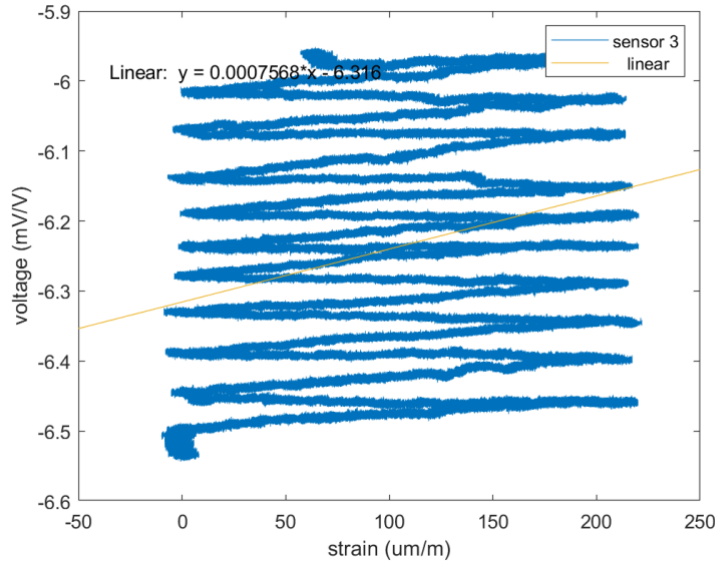


Figure 31: Voltage variation e function of strain of sensor 3

We calculate the gauge factor:

$$GF = \frac{\Delta R_S / R_0}{\Delta L / L_0} = \frac{4R}{R_0} \cdot \frac{\Delta V_{out} / V_{in}}{\Delta L / L_0} = \frac{4 \cdot 10300}{10080} \cdot 0.0007568 \cdot 10^3 = 3.09$$

Comparing the commercial and sensor 3:

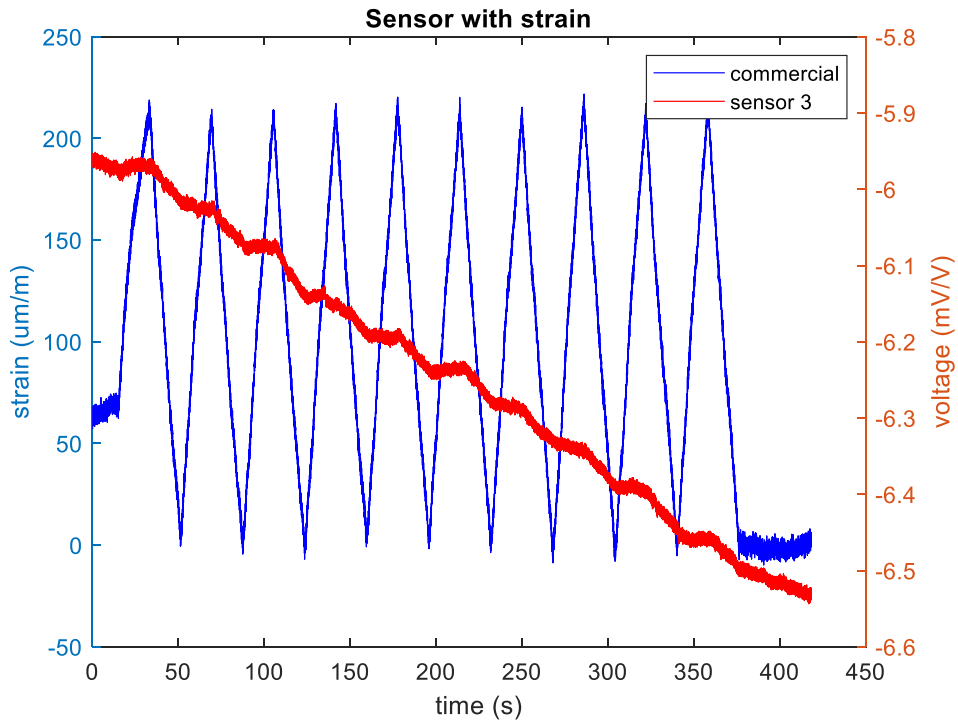


Figure 32: Resistance function of time and strain function of time

Analysis:

In this case, although the strain gauge is high, we can see the problem with this result in the charts. In fact, the variation in resistance with respect to deformation is nearly negligible, making this result unsuitable for our application. Thus, sensor 3 is discarded.

Conclusion

According to the results, sensor 1 is the only one that satisfies the criteria and the one that is going to be used in our application.

9.3. Thermal ageing

Once we have chosen the sensor 1 for our weighing grapple, we still need to do two more tests: thermal ageing and humidity drift.

We do thermal ageing to determine if a preconditioning of sensor 1 is necessary:

- In electronics, sometimes the components such as sensors, are thermal aged to adjust its sensitivity and response to the measured conditions, ensuring it operates within specified parameters.
- Some sensors may experience drift in their measurements over time, as we could see in the temperature and mechanical tests. Thermal aging helps reduce this initial drift, resulting in more stable and accurate readings over time.
- The sensor can be calibrated more precisely, as its properties will have stabilized, resulting in more accurate measurements from the start of its use.

For thermal ageing, a first test is done adjusting the oven to go from -20°C to 80°C and back, at a rate of 1°C per minute and stopping every ten degrees for ten minutes. Nevertheless, it is important to mention that we do not stop in 0 degrees due to it being freezing temperature. Furthermore, we stay for 24 hours in 80°C.

The objective is to see the changes in the initial resistance and to calculate GF again with new initial resistor, which may be decreased as the resistance increases when temperature increases.

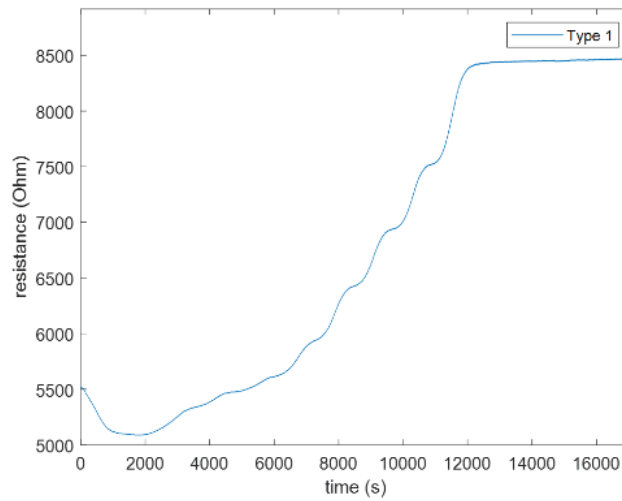


Figure 33: Resistance response to thermal ageing regarding time

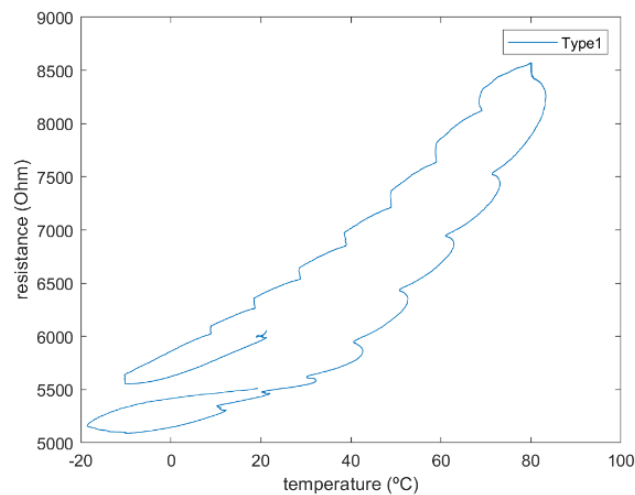


Figure 34: Resistance response to ageing regarding temperature

Calculus of the new gauge factor:

$$GF = \frac{\Delta R_S / R_0}{\Delta L / L_0} = \frac{4R}{R_0} \cdot \frac{\Delta V_{out} / V_{in}}{\Delta L / L_0} = \frac{4 \cdot 5600}{8500} \cdot 0.0005373 \cdot 10^3 = 1.41$$

A second test is also run for 48 hours at 80°C:

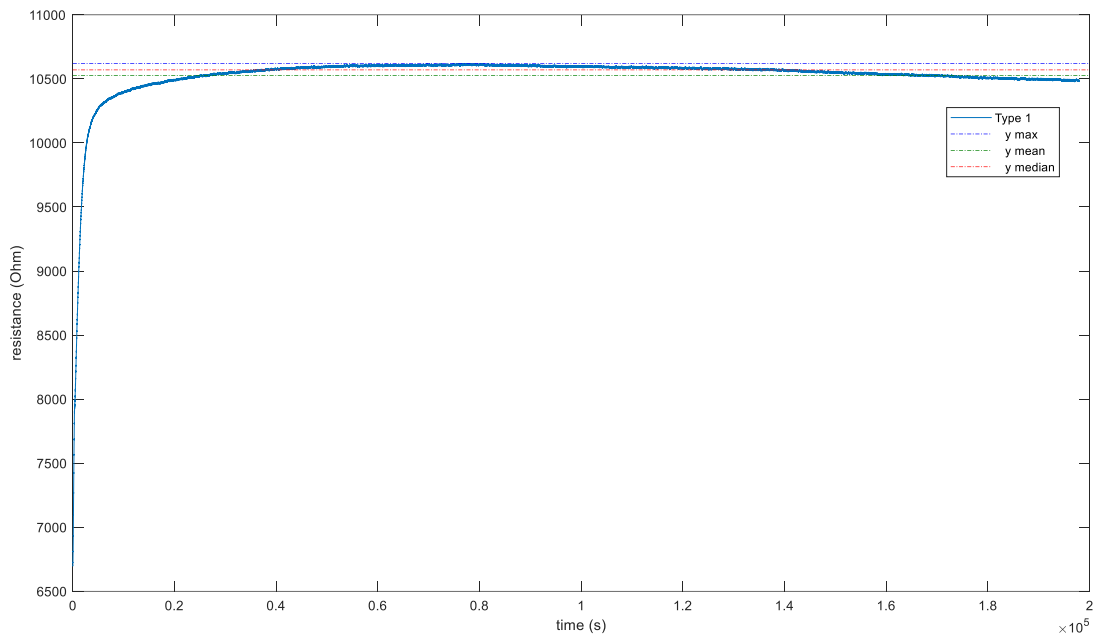


Figure 35: Response to ageing (48 hours at 80°C)

Where: $Y_{max}=10.620 \Omega$ $Y_{mean}=10.530 \Omega$ $Y_{median}=10.570 \Omega$

Calculus of the new gauge factor:

$$GF = \frac{\Delta R_S / R_0}{\Delta L / L_0} = \frac{4R}{R_0} \cdot \frac{\Delta V_{out} / V_{in}}{\Delta L / L_0} = \frac{4 \cdot 5600}{10570} \cdot 0.0005373 \cdot 10^3 = 1.13$$

Conclusion

We can observe an increase of the sensor resistance during the first 11 hours. Afterwards, the resistance stabilizes at approximately 10570 Ω . This could imply that a previous conditioning of the sensor may be performed, this means doing thermal ageing the sensor before use.

Nevertheless, we can see in Figure 34, that there is a decrease on the resistance when the temperature is lowered. The gauge factor significantly decreases with the higher resistance, what we previously expected, making it necessary to compensate the thermal drift in the final design of the printed circuit board.

It interesting to point out that the resistance is bigger at 80°C depending if it has been directly up to this temperature Figure 35 or if it has been increased slowly, like in Figure 33.

We can see that after thermal ageing, there is a decrease of the gauge factor by half, this could be due to the carbon ink layers, the conductivity changes due to ageing, in this case the ink should be investigated more or due to the interface with the dielectric layer of the sensor.

Additionally, more thermal tests could be carried out in order to analyse the evolution of the gauge factor in relation to the different temperatures and to be able to predict its variation and consequently, precisely correct the drift in the final design.

9.4. Humidity drift

A humidity drift test is necessary because humidity might affect the calibration and long-term stability of the sensor, as well as our design of the printed circuit board. Testing helps determine how humidity impacts the sensor's calibration and whether it needs frequent recalibration or if a built-in compensation mechanism is necessary to implement in the PCB.

In other words, humidity testing is a crucial step in ensuring that a sensor performs reliably and accurately in real-world conditions where humidity is a factor. It helps validate the sensor's design, materials, and calibration, ensuring it meets the necessary performance standards for our application.

Ideally, the humidity drift test should be at 85% RH and 40°C for twelve days, in this case the test is going to run for only two days, to see if the relative humidity affects significantly enough to take it into account on the design.

We configurate the humidity chamber (Figure 36):

- Time = 2 days
- Relative humidity = 85%
- Temperature = 40°C



Figure 36: Temperature and humidity chamber



Figure 37: Sensors placed inside the chamber

We obtain the results showed in Figure 38:

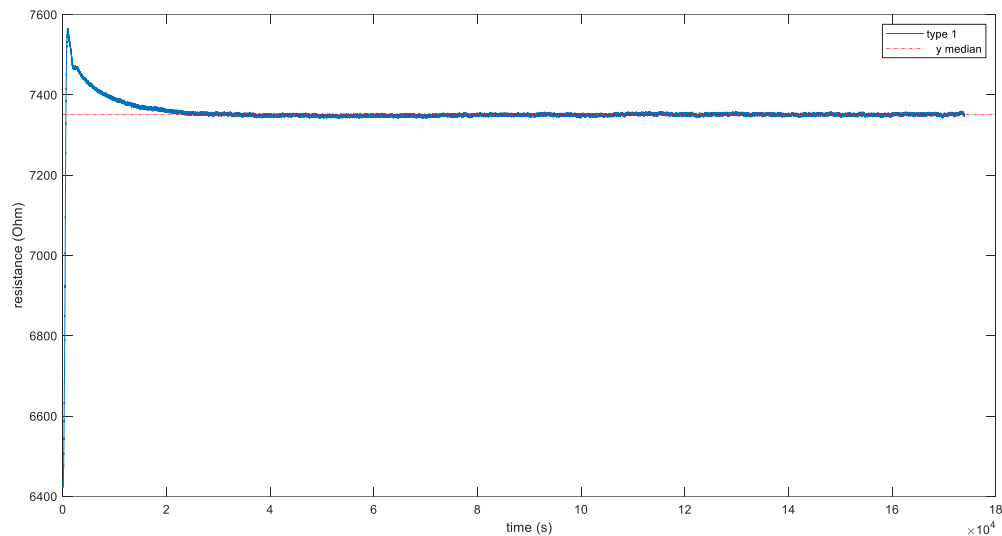


Figure 38: Response of sensor 1 under humidity test

Where Y_{median} is 7350Ω and the response stabilises at almost $30000s \approx 8$ hours.

The sensor shows an important initial sensitivity to humidity, for the first hours, resistance increases for then to be decreased and stabilised around 8 hours.

Considering that the purpose of the sensor is to give real-time weight data, the sensitivity must be addressed in the design of the PCB. We may have various solutions:

- Protect the sensor with a anti humidity coating, minimizing its effects on measurements.
- Implement a compensation system which considers the humidity drift. It must be considered in the microcontroller code of the final design, mitigating the impact of the humidity drift on the sensor response, thereby smoothing its effect in the initial stage of the sensor.
- Do a preconditioning of the sensor with a humidity plus temperature test, as we have seen that the resistance stabilizes after a few hours.

Additionally, we can see from the results of sensors 2 and 3 in Figure 39, the choice of type 1 is proven to be optimal, as we can easily code its humidity drift as first linear and then stabilized. Meanwhile, type 2 still decreases after a long period of hours and type 3 has a lot of oscillations

that are too complex to compensate. This response verifies the correct choice of sensor 1, as it has the best tendency out of the three of them.

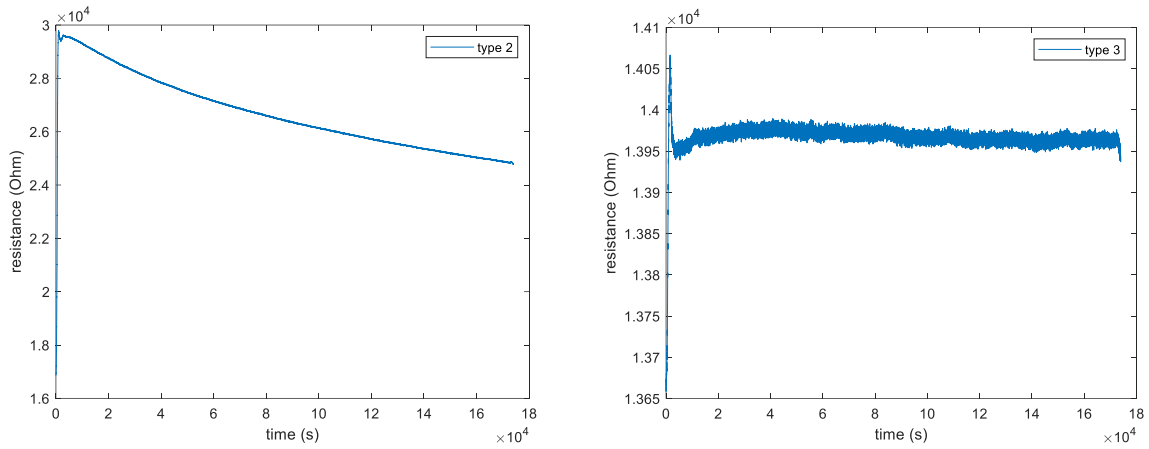


Figure 39: Humidity drift of sensors 2 and 3

On another note, the increase in the resistance is a surprising result, as sensors normally increase their conductivity, so decrease their resistance when they are under humidity conditions. This anomaly should then be studied more, with more future humidity tests, by doing more cycles and testing other values of relative humidity. Also, to determine the compensation component needed.

Chapter 10. Circuit design

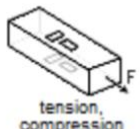
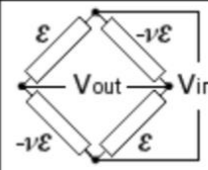
10.1. Schematic

The design must consider the thermal drift of sensor 1. To do so, different components are implemented to fulfil the specifications.

Full bridge configuration

To have a precise measurement and a better thermal drift compensation, we need a full bridge configuration of the sensor. The configuration can be shown in the Table 9 below, that shows how two sensors are placed perpendicularly to the other two, giving respectively the tension and compression of the material, ratio described by Poisson ratio (ν) where:

$$\text{transversal strain} = -\nu \cdot \text{longitudinal strain} (\varepsilon)$$

MEASURES	TYPE	BRIDGE	EQUATION V_{out}/V_{in}	BRIDGE FACTOR	LINEAR	DESCRIPTION
 tension, compression	full		$\frac{k \cdot \varepsilon \cdot (1 + \nu)}{2 + k \cdot \varepsilon \cdot (1 - \nu)}$	$2 \cdot (1 + \nu)$	no	Two pairs of gages where one is in the principal direction and the other one is in transverse direction used in temperature compensation and bending cancellation

ELECTRONICS, PROJECTS, FOCUS (ELPROCUS), TYPES OF STRAIN GAUGE : CHARACTERISTICS & ITS APPLICATIONS

Table 9: characteristics of a full Wheatstone bridge

Amplifier INA8181D

The small signal given by the Wheatstone bridge configuration needs to be amplified to make temperature deviation compensation more effective. This is done with an amplifier INA8181D. In this case, the amplification of the signal, the gain, is conditioned by the resistance chosen in the entrance R1. In this case:

$$\text{Gain} = 1 + \frac{50k}{R1} = 1 + \frac{50k}{78k} = 1.64$$

For the design, we also use the MCP1525T-I/TT to precise a voltage reference of 2.5V in the amplifier.

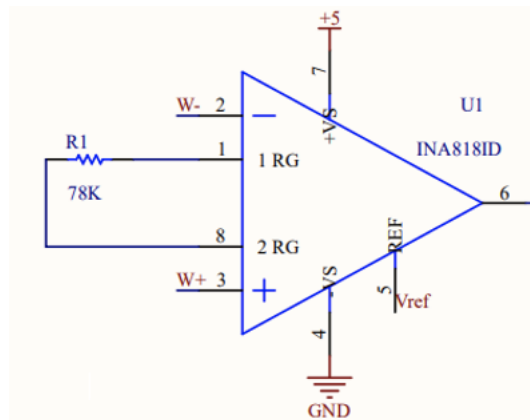
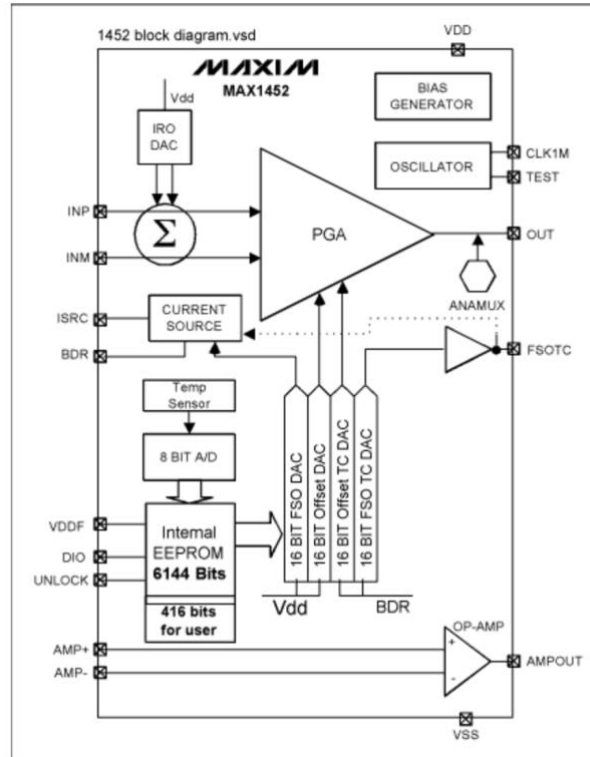


Figure 40: amplifier INA818ID

MAX1452

For thermal drift compensation it is used the component MAX1452 has an internal temperature sensor and an internal microcontroller that adjusts the compensation parameters in real time based on the reading of temperature measured by the sensor. A schema of this component is shown below (Figure 41).



ANALOG DEVICES, DRIVING STRAIN-GAUGE BRIDGE SENSORS WITH SIGNAL-CONDITIONING ICs

Figure 41: internal structure of a MAX1452

Microcontroller ESP32

This MCU was chosen in order to convert, by its internal ADC, the analogic data transmitted by the MAX1452 to digital data. ESP32 has also a radiofrequency output, ideal to then be connected to the module BXee 864MHz of the specifications given by Derisys, that will read the data and then send it to the antenna.

General schematic of the circuit design

Before obtaining the PCB, a schematic design of it is conceived in ALTIUM, where we add and connect the different components.

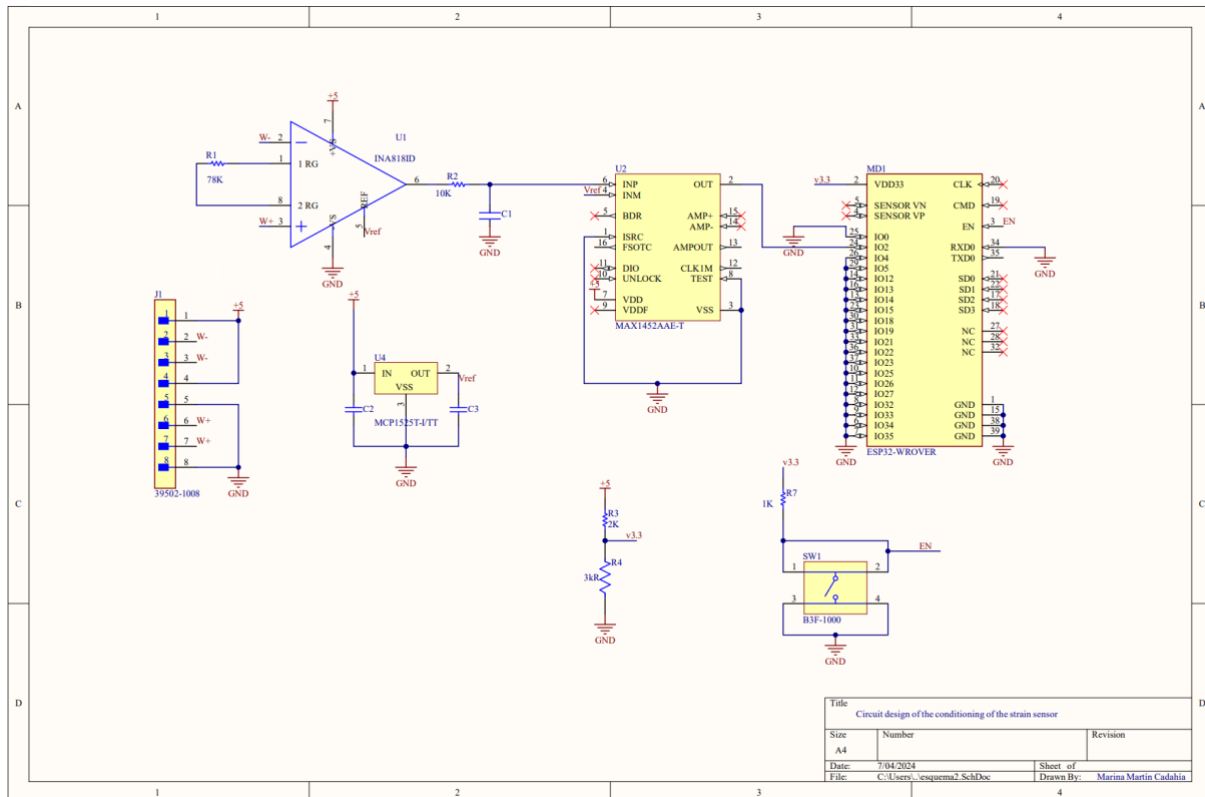


Figure 42: Final schematic design

10.2. PCB design

The schematic is implemented in the making of the printed circuit board, which meets the condition that is located in the usable printing surface (sensor + electronics), a rectangle with dimensions 80x130mm.

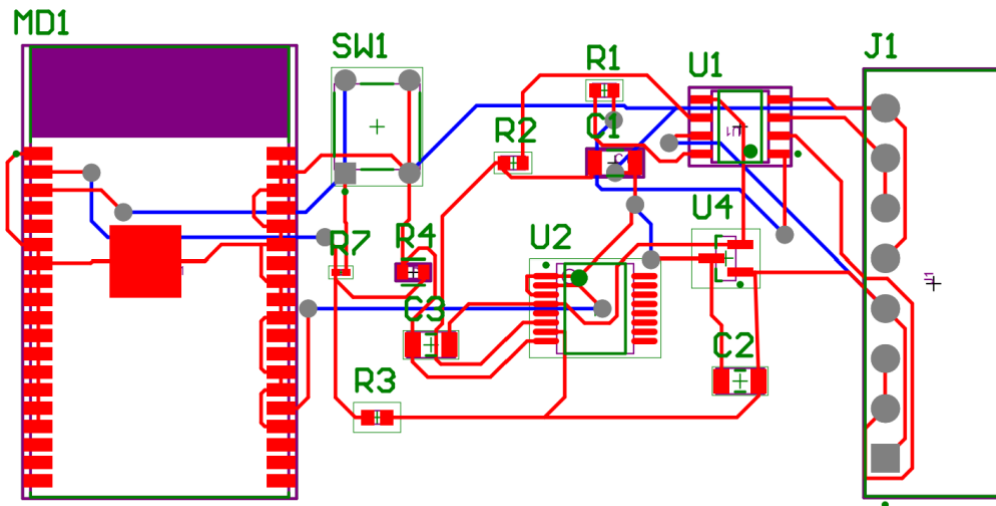


Figure 43: PCB, connection design

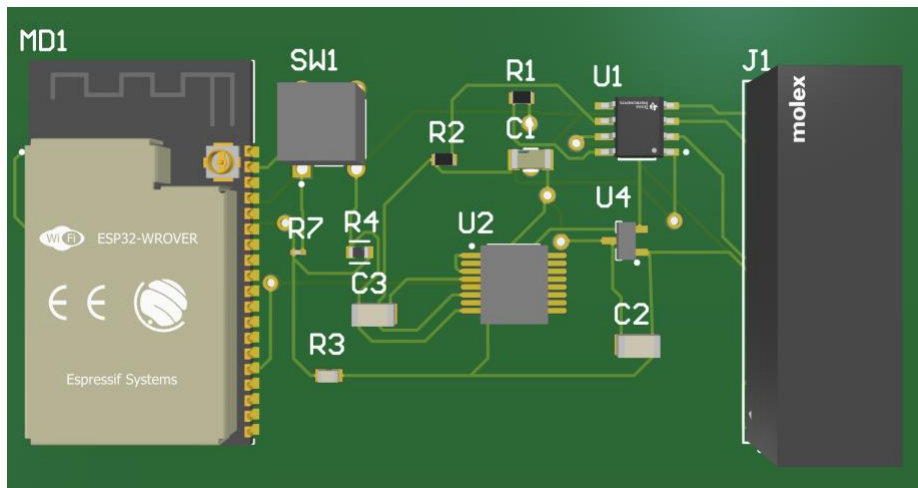


Figure 44: 3D design of the PCB

Chapter 11. Future improvements

Beyond the scope of this project, further features can be implemented to increase the precision of the weighing grapple, that will need to be developed in further stages. Here it is a preliminary list of most relevant points to be taken into consideration:

- a) It is imperative to consider humidity drift in the design. Consequently, more humidity cycles must be carried out, in order to determine the solution, such as the component that will act to compensate the deviation of the resistance regarding humidity.
- b) Further analysis of the gauge factor, obtaining its value for different values of temperatures in thermal ageing.
- c) According to DERISYS specifications, a BXee 868MHz module needs to be added to the design, connected to the ESP32 component. Likewise, an external antenna has to be connected to the BXee to transmit the data to the device that displays the weight taken by the gripper.
- d) The MAX1452 component needs coding that must correspond to the compensation of thermal drift. This coding is done externally, and then implemented in the component by one of its ports (specifically, the one named DIO in Figure 42), that corresponds to the internal EEPROM (Electrically Erasable Programmable Read-Only Memory).
- e) Similarly, the ESP32 needs also coding, bearing in mind that it transforms the analogic data of the MAX1452 to digital data that can be processed by the BXee technology.
- f) To refine the final PCB design to optimize the location of the new components.

Chapter 12. Conclusion

Screen printing allows a more efficient and optimal design of a weighing grapple. The test results show the utility of sensor 1, that is the chosen one to do the PCB, as it offers an adequate strain gauge, of value around 2.2, the same as metallic strain sensors. From the tests, we should consider a few aspects of this sensor:

- Its dependency to temperature makes it compulsory to treat the temperature variation with the component MAX1452, which acts to compensate the drift.
- The stabilization of the sensor resistance after the ageing test, so might be a good option to do a preconditioning process, to achieve this stabilization for an optimal performance of the sensor.
- A stabilization after a few hours in the humidity test, which can also be taken into consideration for the preconditioning of the sensor.

For personal perspective, it has been an exceptional opportunity to participate in a genuine real engineering project and to understand the various stages involved, from identifying an issue, such as the inefficiency of an S-sensor, to the proposal of a solution. Additionally, it has provided insight into the procedural steps, including the numerous tests that require considerable trial and error and time to determine the appropriate adjustments for achieving satisfactory results.

Furthermore, this experience offers the chance to learn about advanced technologies such as screen printing in printed electronics, which represent significant progress toward future innovations and the optimization and enhancement of product efficiency. This is, ultimately, the primary objective of engineering.

Chapter 13. Bibliography

[BEST24] Bestech Australia: Sensors and teaching equipment. Last accessed on 12/07/2024. <https://www.bestech.com.au/blogs/understanding-a-wheatstone-bridge-strain-gauge-circuit/>

[RECT24] Recycling today, RMT-XW Grapple Scales. Last accessed on 12/07/2024. <https://www.recyclingtoday.com/product/rmt-xw-grapple-scales/>

[REPN11] Recycling Product News, Wireless grapple scale allows scrap operations to add in-motion weigh capacity, RMT, wireless grapple scale, scrap recycling, in-motion weighing. March, 2011. Last accessed on 12/07/2024. <https://www.recyclingproductnews.com/article/1204/wireless-grapple-scale-allows-scrap-operations-to-add-in-motion-weigh-capacity>

[WEIS24] Weiss Technik, Temperature test chambers, type TempEvent. Search date: March 2024. Last accessed on 12/07/2024. <https://www.weiss-technik.com/en/products/detail/temperature-test-chambers-type-tempevent~p27474>

[MGFE24] McGill Formula Electric, Compact Strain Gauge Board for MFE22, Canada. April 2022. Last accessed on 12/07/2024. <https://www.hackster.io/MFE/compact-strain-gauge-board-for-mfe22-113dd5>

[ANAL04] Analog Devices, Driving Strain-Gauge Bridge Sensors with Signal-Conditioning ICs. December 2004. Last accessed on 12/07/2024. <https://www.analog.com/en/resources/technical-articles/driving-straingauge-bridge-sensors-with-signalconditioning-ics.html>

[ELPR24] Electronics, Projects, Focus (ELPROCUS), Types of Strain Gauge : Characteristics & Its Applications. Last accessed on 12/07/2024. <https://www.elprocus.com/types-of-strain-gauge/>

[YANM24] Yanmis, S Type Pressure Sensor, Portable S Type Beam Load Cell Scale Sensor Weighting Sensor 500kg for Hopper Weight High Pressure Tension Weighing, Amazon. Last accessed on 12/07/2024. <https://www.amazon.com/Pressure-Portable-Weighting-Tension-Weighing/dp/B07TKGZW7S>

[QUAD23] Quad Industries, Screen printing for electronics: an overview, screen printing, Technology. May 2023. Last accessed on 12/07/2024. <https://www.quad-ind.com/screen-printing-for-electronics-an-overview/>

[SHIM24] Shimadzu, Autograph AGS-X Series. Last accessed on 12/07/2024. <https://www.shimadzu.com/an/industries/engineering-materials/metal/tensile-test/index.html>

[PRIM23] Primoz Rome, Dewesoft, New Sirius UNI Universal strain gauge, IEPE, Voltage, RTD, resistance and current amplifier. February 2023. Last accessed on 12/07/2024. <https://dewesoft.com/es/blog/amplificador-sirius-uni-universal>

